

## **STUDY OF HALL CURRENT EFFECTS ON MHD FLOW IN ROTATING SYSTEM THROUGH POROUS MEDIUM**

---

Importance of Hall current effect on MHD flow in rotating system is considered in present investigation, which is not discussed in previous literature. Study of MHD flow in a rotating system has attracted several investigators due to its various applications in many areas of science and technology. The MHD rotating flow of an electrically conducting fluid is encountered in geophysical fluid dynamics, solar physics dealing with the sunspot development, the solar cycle and the structure of rotating magnetic stars. In this concern, researchers may mention the works done by Rapits [165]. Many works of plasma physics, Hall current effects have not received much attention. Development of an additional potential variance between opposite surfaces of a conductor for which a current is induced perpendicular to both the electric and magnetic field. This current is called as Hall current, which is first introduced by Hall [14]. Narayana et al. [130] and Olajuwon et al. [132] discussed radiation and Hall current effects on MHD flow of micro-polar fluid.

This chapter comprises of two sections, effects of radiation and chemical reaction on unsteady MHD Casson fluid flow through porous medium considering heat generation and Hall effects in rotating system are discussed in first section. Work discussed in first section is extended in second section by considering Soret and Hall current effects on exponentially accelerated vertical plate.

### **7.1 SECTION I: HEAT GENERATION/ABSORPTION AND HALL EFFECTS ON MHD CASSON FLUID FLOW PAST AN OSCILLATING VERTICAL PLATE WITH RAMPED WALL TEMPERATURE IN ROTATING SYSTEM THROUGH POROUS MEDIUM**

The present section is concerned with the study of heat generation/absorption and Hall effects on Casson fluid flow in presence of magnetic field past an oscillating vertical plate in rotating system with ramped boundary conditions. Governing non-dimensional equations are solved using Laplace transform technique and obtained expression for primary velocity, secondary velocity, temperature and concentration profiles. In order to understand effects of ramped boundary conditions, the solution of said problem is obtained for isothermal boundary conditions. For both boundary conditions, the numerical values of primary velocity, secondary velocity, temperature and concentration profiles are presented graphically for several values of the pertinent parameters. Expression for Skin friction, Nusselt number and Sherwood number are derived and presented in tabular form.

### 7.1.1 INTRODUCTION

The rotating flow of an electrically conducting fluid in presence of magnetic field has got its importance in Geophysical problems. The study of rotating flow problems is also important in the solar physics dealing with the sunspot development, the solar cycle and the structure of rotating magnetic stars. Raptis and Singh [136] discussed rotation effects on fluid flow in presence of magnetic field past an accelerated vertical plate. Rashidi et al. [137] investigated entropy generation in slip flow over a rotating disk, whereas Rashidi and Erfani [138] obtained analytical solution of steady MHD convective and slip flow due to a rotating disk. Hall effects on MHD flow in rotating system has many applications in science and technology. It plays an important role in determining flow structures because it induces secondary flow in the flow-field (Sherman and Sutton [166]). Recently, Seth et al. [133-134] discussed effects of Hall current and rotation on natural convection flow past a moving vertical plate. Hussain et al. [135] studied Hall effects, heat absorption and chemical reaction over an accelerated moving plate in a rotating system. Seth et al. [142] considered thermal radiation, rotation on MHD flow with ramped wall temperature whereas, Seth et al. [144-145] studied heat generation and Hall current effects on MHD flow through porous medium with ramped wall temperature.

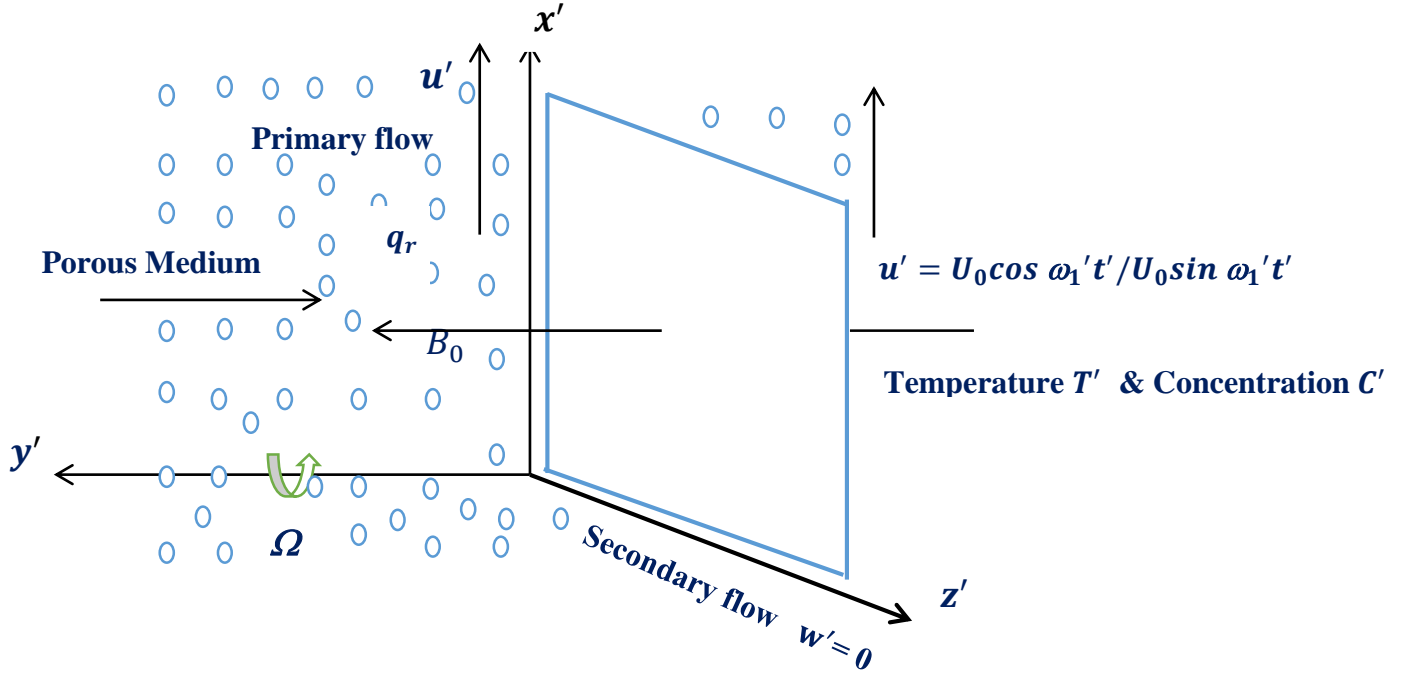
### 7.1.2 Novelty of the Problem

Purpose of this section is to investigate Hall current and heat generation effects on time dependent MHD flow of Casson fluid past an oscillating vertical plate. System under consideration is rotating with ramped wall temperature. The governing dimensionless equations with imposed initial boundary are solved using Laplace transform technique. The acquired solutions are in agreement with earlier work are shown through tabular forms. Such study may find application in fire dynamics in insulations and geothermal energy systems etc.

### 7.1.3 Mathematical Formulation of the Problem

Coordinate system is such that  $x'$  – axis is along the plate,  $y'$  – axis is normal to it and  $z'$  is perpendicular to  $x'y'$  plane as shown in Figure 7.1.1. Fluid and plate are rotate anticlockwise with angular velocity  $\Omega$  about  $y'$  – axis. Initially, at time  $t' \leq 0$ , fluid and the plate are at constant temperature  $T'_{\infty}$  and concentration  $C'_{\infty}$ . At time  $t' > 0$ , the plate is oscillate in  $x'$  – axis direction against gravitational field with velocity  $U_0 \cos(\omega_1 t')$ . At the time  $t' > 0$ , temperature of the wall

is instantaneously raised or lowered to  $T'_\infty + (T'_w + T'_\infty) t'/t_0$  when  $t' \leq t_0$  and  $T'_w$  when  $t' > t_0$  which is there after maintained constant  $T'_w$ . The level of surface concentration is raised linearly to  $C'_\infty + (C'_w - C'_\infty) t'/t_0$  which is there after maintained constant  $C'_w$ . It is assumed that the effects of viscous dissipation, induced magnetic and electrical field are negligible.



$$T' = \begin{cases} T'_\infty + (T'_w - T'_\infty) t'/t_0 & \text{if } 0 < t' < t_0 \\ T'_w & \text{if } t' \geq t_0 \end{cases}, C' = C'_\infty + (C'_w - C'_\infty) t'/t_0; y' = 0$$

Figure 7.1.1: Physical Sketch of the Problem

Under above assumptions and taking into account the Boussinesq approximation, governing equations are given below:

$$\rho \frac{\partial u'}{\partial t'} + 2\Omega w' = \mu B \left(1 + \frac{1}{\gamma}\right) \frac{\partial^2 u'}{\partial y'^2} - \frac{\sigma B_0^2}{(1+m^2)} (u' + mw') - \frac{\mu B}{k'} u' + g\rho\beta'_T (T' - T'_\infty) + g\rho\beta'_C (C' - C'_\infty) \quad (7.1.1)$$

$$\rho \frac{\partial w'}{\partial t'} - 2\Omega u' = \mu B \left(1 + \frac{1}{\gamma}\right) \frac{\partial^2 w'}{\partial y'^2} - \frac{\sigma B_0^2}{(1+m^2)} (mu' - w') - \frac{\mu B}{k'} u' \quad (7.1.2)$$

$$\frac{\partial T'}{\partial t'} = \frac{k_4}{\rho c_p} \frac{\partial^2 T'}{\partial y'^2} - \frac{1}{\rho c_p} \frac{\partial q_r'}{\partial y'} + \frac{Q_0}{\rho c_p} (T' - T'_\infty) \quad (7.1.3)$$

$$\frac{\partial C'}{\partial t'} = D_M \frac{\partial^2 C'}{\partial y'^2} - k'_2 (C' - C'_\infty) \quad (7.1.4)$$

with following initial and boundary conditions:

$$u' = 0, w' = 0 \quad T' = T'_\infty, C' = C'_\infty; \text{ as } y' \geq 0 \text{ and } t' \leq 0 \quad (7.1.5)$$

$$u' = U_0 \cos \omega_1 t', w' = 0, T' = \begin{cases} T'_\infty + (T'_w - T'_\infty) t'/t_0 & \text{if } 0 < t' < t_0, \\ T'_w & \text{if } t' \geq t_0 \end{cases},$$

$$C' = C'_\infty + (C'_w - C'_\infty) t'/t_0; \quad t' \geq 0 \text{ and } y' = 0, \quad (7.1.6)$$

$$u' \rightarrow 0, T' \rightarrow T'_\infty, C' \rightarrow C'_\infty; \text{ as } y' \rightarrow \infty \text{ and } t' \geq 0 \quad (7.1.7)$$

Using the Rosseland approximation [91], the radiative heat flux term is given by.

$$\frac{\partial q_r'}{\partial y'} = - \frac{16\sigma^* T_\infty'^3}{3k^*} \frac{\partial^2 T'}{\partial y'^2} \quad (7.1.8)$$

Using equations (7.1.8) in equation (7.1.3),

$$\frac{\partial T'}{\partial t'} = \frac{k_4}{\rho c_p} \frac{\partial^2 T'}{\partial y'^2} + \frac{1}{\rho c_p} \frac{16\sigma^* T_\infty'^3}{3k^*} \frac{\partial^2 T'}{\partial y'^2} + \frac{Q_0}{\rho c_p} (T' - T'_\infty) \quad (7.1.9)$$

Introducing the following dimensionless quantities

$$y = \frac{y'}{U_0 t_0}, \quad u = \frac{u'}{U_0}, \quad t = \frac{t'}{t_0}, \quad \theta = \frac{(T' - T'_\infty)}{(T'_w - T'_\infty)}, \quad C = \frac{(C' - C'_\infty)}{(C'_w - C'_\infty)}$$

$$\frac{\partial u}{\partial t} + 2k_1^2 w = \left(1 + \frac{1}{\gamma}\right) \frac{\partial^2 u}{\partial y^2} - \frac{M^2}{1+m^2} (u + mw) - \frac{1}{k_1} u + G_r \theta + G_m C \quad (7.1.10)$$

$$\frac{\partial w}{\partial t} - 2k_1^2 u = \left(1 + \frac{1}{\gamma}\right) \frac{\partial^2 w}{\partial y^2} + \frac{M^2}{1+m^2} (mu - w) - \frac{1}{k_1} w \quad (7.1.11)$$

$$\frac{\partial \theta}{\partial t} = \frac{1+Nr}{Pr} \frac{\partial^2 \theta}{\partial y^2} + H\theta \quad (7.1.12)$$

$$\frac{\partial C}{\partial t} = \frac{1}{s_c} \frac{\partial^2 C}{\partial y^2} - krC \quad (7.1.13)$$

with initial and boundary condition

$$u = w = \theta = C = 0, \quad y \geq 0, t \leq 0$$

$$u = \cos(\omega_1 t), w = 0, \quad \theta = \begin{cases} t, & 0 < t \leq 1 \\ 1 & t > 1 \end{cases} = tH(t) - (t-1)H(t-1),$$

$$C = t \text{ at } y = 0, t > 0$$

$$u \rightarrow 0, w \rightarrow 0, \theta \rightarrow 0, C \rightarrow 0 \text{ at } y \rightarrow \infty, t > 0 \quad (7.1.14)$$

Using  $F = u + iw$  in equations 7.1.10 and 7.1.11,

$$\frac{\partial F}{\partial t} + \left(\frac{M^2(1-im)}{1+m^2} + \frac{1}{k_1} - 2ik_1^2\right) F = \left(1 + \frac{1}{\gamma}\right) \frac{\partial^2 F}{\partial y^2} + G_r \theta + G_m C \quad (7.1.15)$$

$$\frac{\partial \theta}{\partial t} = \frac{1+Nr}{Pr} \frac{\partial^2 \theta}{\partial y^2} + H\theta \quad (7.1.16)$$

$$\frac{\partial C}{\partial t} = \frac{1}{s_c} \frac{\partial^2 C}{\partial y^2} - krC \quad (7.1.17)$$

with initial and boundary condition

$$F = \theta = C = 0, \quad y \geq 0, t \leq 0$$

$$F = C \cos \omega_1 t, \quad \theta = \begin{cases} t, & 0 < t \leq 1 \\ 1, & t > 1 \end{cases} = tH(t) - (t-1)H(t-1), C = t \text{ at } y = 0, t > 0$$

$$F \rightarrow 0, \theta \rightarrow 0, C \rightarrow 0 \text{ at } y \rightarrow \infty, t > 0 \quad (7.1.18)$$

Where,

$$Gr = \frac{\nu g \beta'_T (T'_w - T'_\infty)}{U_0^3}, Gm = \frac{\nu g \beta'_C (C'_w - C'_\infty)}{U_0^3}, M = \frac{\sigma B_0^2 \nu}{\rho U_0^2}, Pr = \frac{\rho \nu C_p}{k_4}, Nr = \frac{16 \sigma^* T_\infty'^3}{3 k_4 k^*},$$

$$H = \frac{Q_0 \nu^2}{k_4 U_0^2}, Sc = \frac{\nu}{D_M}, Kr = \frac{\nu k_2'}{U_0^2}, k = \frac{\nu \phi}{k'}$$

### 7.1.4 Solution of the Problem

Governing system of equations (7.1.15) to (7.1.17) with imposed initial and boundary conditions (7.1.18) are solved using the Laplace transform.

#### 7.1.4.1 Solution of the problem for ramped wall temperature and ramped surface concentration

$$\theta(y, t) = f_2(y, t, -H, a_2) - f_2(y, t-1, -H, a_2)H(t-1) \quad (7.1.19)$$

$$C(y, t) = f_2(y, t, Kr, a_3) \quad (7.1.20)$$

$$F(y, t) = \frac{1}{2} f_3(y, t, a_1, a, iw) + \frac{1}{2} f_3(y, t, a_1, a, -iw) + f_4(y, t, a_1, a, -a_6) - f_4(y, t - 1, a_1, a, -a_6)H(t-1) + f_5(y, t, a_1, a, a_{10}) - f_4(y, t, -H, a_2, -a_6) + f_4(y, t - 1, -H, a_2, -a_6)H(t-1) - f_5(y, t, Kr, a_3, a_{10}) \quad (7.1.21)$$

#### 7.1.4.2 Solution of the problem for isothermal temperature and ramped surface concentration

In this case, the initial and boundary conditions are the same excluding Eq. (7.1.18) that becomes  $\theta = 1$  at  $y = 0, t \geq 0$ . So, The governing expression of  $\theta(y, t), C(y, t)$  and  $F(y, t)$  for isothermal temperature are given below.

$$\theta(y, t) = f_1(y, t, -H, a_2) - f_2(y, t-1, -H, a_2)H(t-1) \quad (7.1.22)$$

$$C(y, t) = f_2(y, t, Kr, a_3) \quad (7.1.23)$$

$$F(y, t) = \frac{1}{2} f_3(y, t, a_1, a, iw) + \frac{1}{2} f_3(y, t, a_1, a, -iw) + f_6(y, t, a_1, a, -a_6) + f_5(y, t, a_1, a, a_{10}) - f_6(y, t, -H, a_2, -a_6) - f_5(y, t, Kr, a_3, a_{10}) \quad (7.1.24)$$

where,

$$f_1(y, t, a, b) = L^{-1} \left( \frac{e^{-y\sqrt{\frac{s+a}{b}}}}{s} \right) = \frac{1}{2} \left[ e^{-y\sqrt{\frac{a}{b}}} \operatorname{erfc} \left( \frac{y}{2\sqrt{bt}} - \sqrt{at} \right) + e^{y\sqrt{\frac{a}{b}}} \operatorname{erfc} \left( \frac{y}{2\sqrt{bt}} + \sqrt{at} \right) \right] \quad (7.1.25)$$

$$f_2(y, t, a, b) = L^{-1} \left( \frac{e^{-y\sqrt{\frac{s+a}{b}}}}{s^2} \right) = \frac{1}{2} \left[ \left( t - \frac{y}{2\sqrt{ab}} \right) e^{-y\sqrt{\frac{a}{b}}} \operatorname{erfc} \left( \frac{y}{2\sqrt{bt}} - \sqrt{at} \right) + \left( t + \frac{y}{2\sqrt{ab}} \right) e^{y\sqrt{\frac{a}{b}}} \operatorname{erfc} \left( \frac{y}{2\sqrt{bt}} + \sqrt{at} \right) \right] \quad (7.1.26)$$

$$f_3(y, t, a, b, c) = L^{-1} \left( \frac{e^{-y\sqrt{\frac{s+a}{b}}}}{(s+c)} \right) = \frac{e^{-ct}}{2} \left[ e^{-y\sqrt{\frac{1}{b}(a-c)}} \operatorname{erfc} \left( \frac{y}{2\sqrt{bt}} - \sqrt{(a-c)t} \right) + e^{y\sqrt{\frac{1}{b}(a-c)}} \operatorname{erfc} \left( \frac{y}{2\sqrt{bt}} + \sqrt{(a-c)t} \right) \right] \quad (7.1.27)$$

$$f_4(y, t, a, b, c) = a_{14}f_1(y, t, a, b) + a_{12}f_2(y, t, a, b) + a_{13}f_3(y, t, a, b, c) \quad (7.1.28)$$

$$f_5(y, t, a, b, c) = a_{17}f_1(y, t, a, b) + a_{15}f_2(y, t, a, b) + a_{16}f_3(y, t, a, b, c) \quad (7.1.29)$$

$$f_6(y, t, a, b, c) = a_{12}f_1(y, t, a, b) - a_{12}f_2(y, t, a, b, c) \quad (7.1.30)$$

### 7.1.4.3 Skin friction, Nusselt number and Sherwood number

Expressions of skin-friction  $\tau = \tau_x + i\tau_z$ , Nusselt number  $Nu$  and Sherwood number  $Sh$  for ramped wall temperature and isothermal temperature are calculated from the equations (7.1.19) to (7.1.24) using the relations

$$\tau^*(y, t) = -\mu_B \left( 1 + \frac{1}{\gamma} \right) \tau \quad \text{Where} \quad \tau = \left. \frac{\partial f}{\partial y} \right|_{y=0}, \quad Nu = -\left. \left( \frac{\partial \theta}{\partial y} \right) \right|_{y=0}, \quad Sh = -\left. \left( \frac{\partial C}{\partial y} \right) \right|_{y=0} \quad (7.1.31)$$

For ramped wall temperature and ramped surface concentration

$$\tau(y, t) = \frac{1}{2}I_3(t, a_1, a, i\omega) + \frac{1}{2}I_3(t, a_1, a, -i\omega) + I_4(t, a_1, a, -a_6) - I_4(t-1, a_1, a, -a_6)H(t-1) + I_5(t, a_1, a, a_{10}) - I_4(t, -H, a_2, -a_6) + I_4(t-1, H, a_2, -a_6)H(t-1) - I_5(t, Kr, a_3, a_{10}) \quad (7.1.32)$$

$$Nu = -[I_2(t, -H, a_2) - I_2(t-1, -H, a_2)H(t-1)] \quad (7.1.33)$$

$$Sh = -[I_2(t, Kr, a_3)] \quad (7.1.34)$$

For isothermal temperature and ramped surface concentration

$$\tau(y, t) = \frac{1}{2}I_3(t, a_1, a, i\omega) + \frac{1}{2}I_3(t, a_1, a, -i\omega) + I_6(t, a_1, a, -a_6) + I_5(t, a_1, a, a_{10}) - I_6(t, -H, a_2, -a_6) - I_5(t, Kr, a_3, a_{10}) \quad (7.1.35)$$

$$Nu = -[I_1(t, -H, a_2)] \quad (7.1.36)$$

$$Sh = -[I_2(t, Kr, a_3)] \quad (7.1.37)$$

Where,

$$I_1(t, a, b) = \left. \frac{df_1(y, t, a, b)}{dy} \right|_{y=0} = -\sqrt{\frac{a}{b}} \operatorname{erf}(\sqrt{at}) - \frac{e^{-at}}{\sqrt{\pi bt}} \quad (7.1.38)$$

$$I_2(t, a, b) = \left. \frac{df_2(y, t, a, b)}{dy} \right|_{y=0} = -\frac{1}{\sqrt{4ab}} \operatorname{erf}(\sqrt{at}) - t\sqrt{\frac{a}{b}} \operatorname{erf}(\sqrt{at}) - \sqrt{\frac{t}{\pi b}} e^{-at} \quad (7.1.39)$$

$$I_3(t, a, b, c) = \left. \frac{df_3(y, t, a, b, c)}{dy} \right|_{y=0} = -e^{-ct} \sqrt{\frac{a-c}{b}} \operatorname{erf}(\sqrt{(a-c)t}) - \frac{e^{-at}}{\sqrt{\pi bt}} \quad (7.1.40)$$

$$I_4(t, a, b) = \left. \frac{df_4(y, t, a, b, c)}{dy} \right|_{y=0} = a_{14}I_1(t, a, b) + a_{12}I_2(t, a, b) + a_{13}I_3(t, a, b, c) \quad (7.1.41)$$

$$I_5(t, a, b) = \left. \frac{df_5(y, t, a, b, c)}{dy} \right|_{y=0} = a_{17}I_1(t, a, b) + a_{15}I_2(t, a, b) + a_{16}I_3(t, a, b, c) \quad (7.1.42)$$

$$I_6(t, a, b) = \left. \frac{df_6(y, t, a, b, c)}{dy} \right|_{y=0} = a_{12}I_1(t, a, b) - a_{12}I_2(t, a, b, c) \quad (7.1.43)$$

### 7.1.5 Result and Discussion

Effects of Hall current  $m$ , rotation  $K_1$ , magnetic field  $M$ , permeability of porous medium  $k$ , Casson fluid parameter  $\gamma$ , Chemical reaction  $Kr$ , thermal radiation  $Nr$  and heat generation  $H$  on primary velocity, secondary velocity, temperature and concentration profiles are presented in Figure 7.1.2 to 7.1. 18. It is revealed from Figure 7.1.2 to Figure 7.1.18 that, for both thermal plates, primary velocity, secondary velocity, temperature and concentration profiles attain a distinctive maximum value near surface of the plate and then decrease appropriately on increasing boundary layer coordinate  $y$  to approach free stream value. Figure 7.1.2 to Figure 7.1.3 depict the effect of Hall current  $m$  on primary and secondary fluid velocities for ramped wall temperature and isothermal temperature. It is revealed from Figure 7.1.2 and Figure 7.1.3 that, for both thermal plates, Hall current tends to accelerate fluid flow in both flow directions. Physically, Hall current tends to induce Secondary flow in the flow field. Due to this effect, it is observed from Figure 7.1.2 and Figure 7.1.3 that motion of the fluid flow in secondary flow direction is more than that motion of the fluid in primary flow direction.

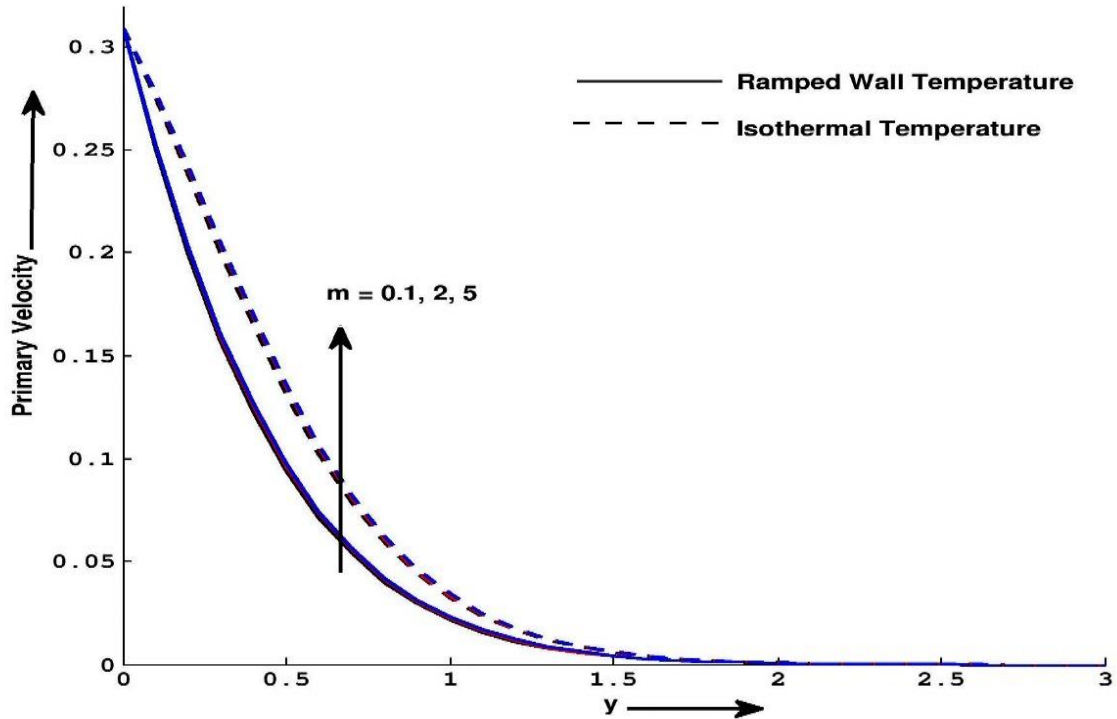


**Figure 7.1.2:** Primary Velocity profile  $u$  for different values of  $y$  and  $m$  at  $\gamma = 1, M = 1, k = 0.5, k_1 = 2, Pr = 15, Sc = 6.2, H = 5, Gm = 2, Gr = 3, Nr = 3, Kr = 5, \omega_1 = \frac{\pi}{2}$  and  $t = 0.2$

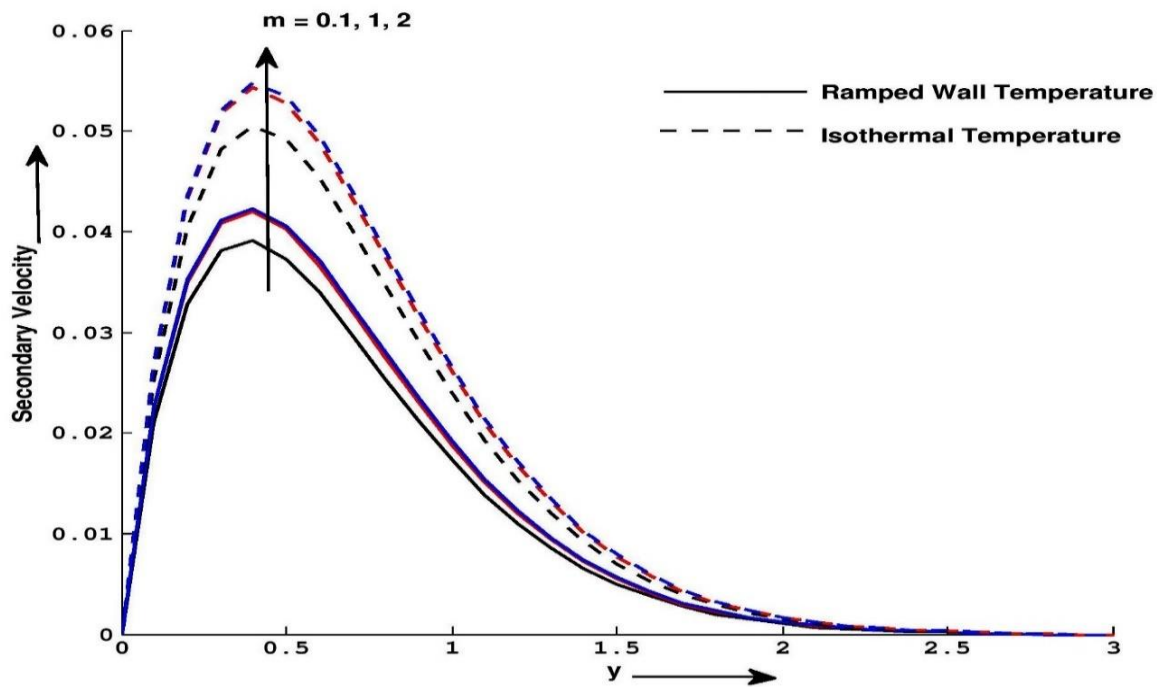


**Figure 7.1.3:** Secondary Velocity profile  $w$  for different values of  $y$  and  $m$  at  $\gamma = 1, M = 1, k = 0.5, k_1 = 2, Pr = 15, Sc = 6.2, H = 5, Gm = 2, Gr = 3, Nr = 3, Kr = 5, \omega_1 = \frac{\pi}{2}$  and  $t = 0.2$

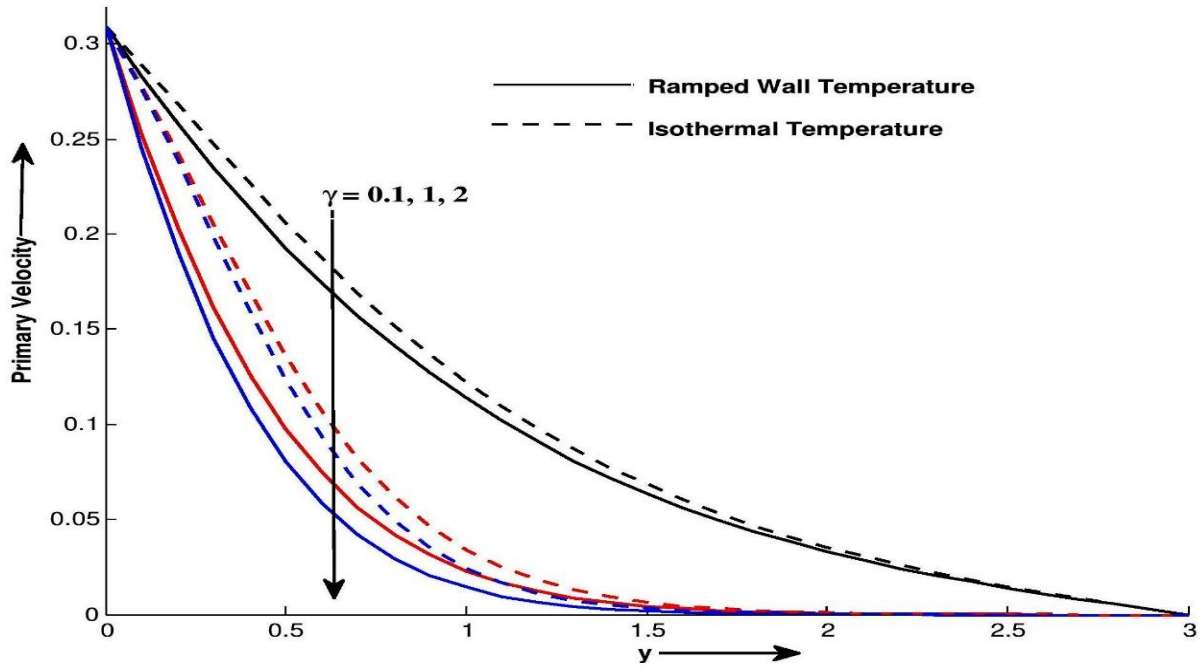


**Figure 7.1.4:** Primary Velocity profile  $u$  for different values of  $y$  and  $\gamma$  at  $m = 5, M = 1, k = 0.5, k_1 = 2, Pr = 15, Sc = 6.2, H = 5, Gm = 2, Gr = 3, Nr = 3, Kr = 5, \omega_1 = \frac{\pi}{2}$  and  $t = 0.2$

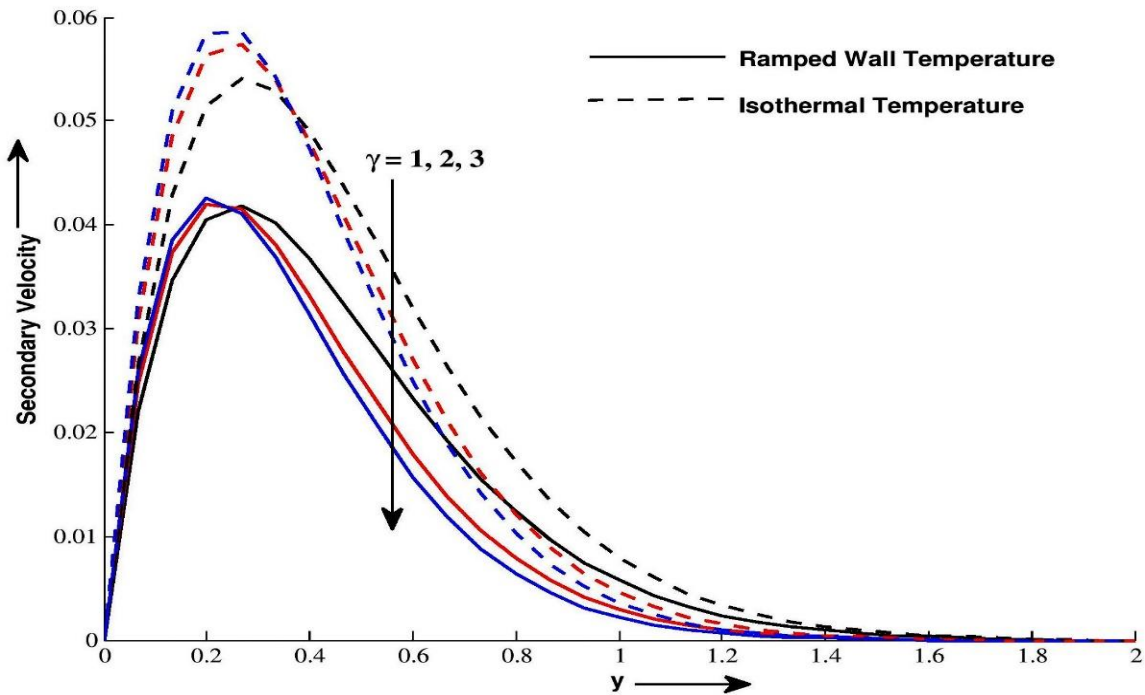


**Figure 7.1.5:** Secondary Velocity profile  $w$  for different values of  $y$  and  $\gamma$  at  $m = 5, M = 1, k = 0.5, k_1 = 2, Pr = 15, Sc = 6.2, H = 5, Gm = 2, Gr = 3, Nr = 3, Kr = 5, \omega_1 = \frac{\pi}{2}$  and  $t = 0.2$

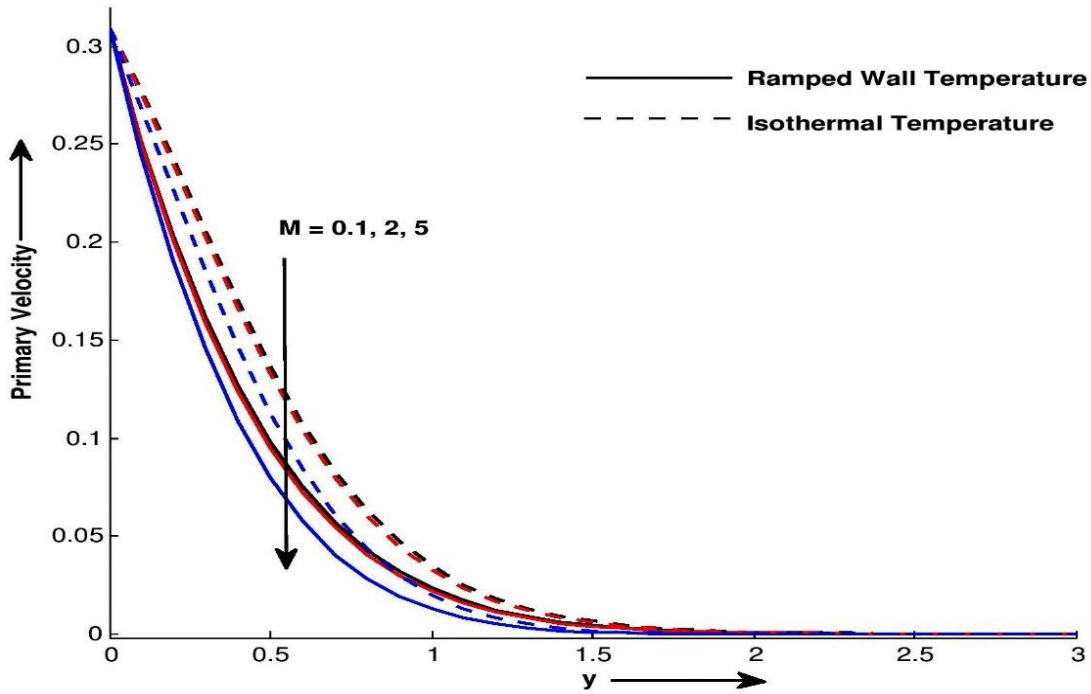


**Figure 7.1.6:** Primary Velocity profile  $u$  for different values of  $y$  and  $M$  at  $\gamma = 1, m = 5, k = 0.5, k_1 = 2, Pr = 15, Sc = 6.2, H = 5, Gm = 2, Gr = 3, Nr = 3, Kr = 5, \omega_1 = \frac{\pi}{2}$  and  $t = 0.2$

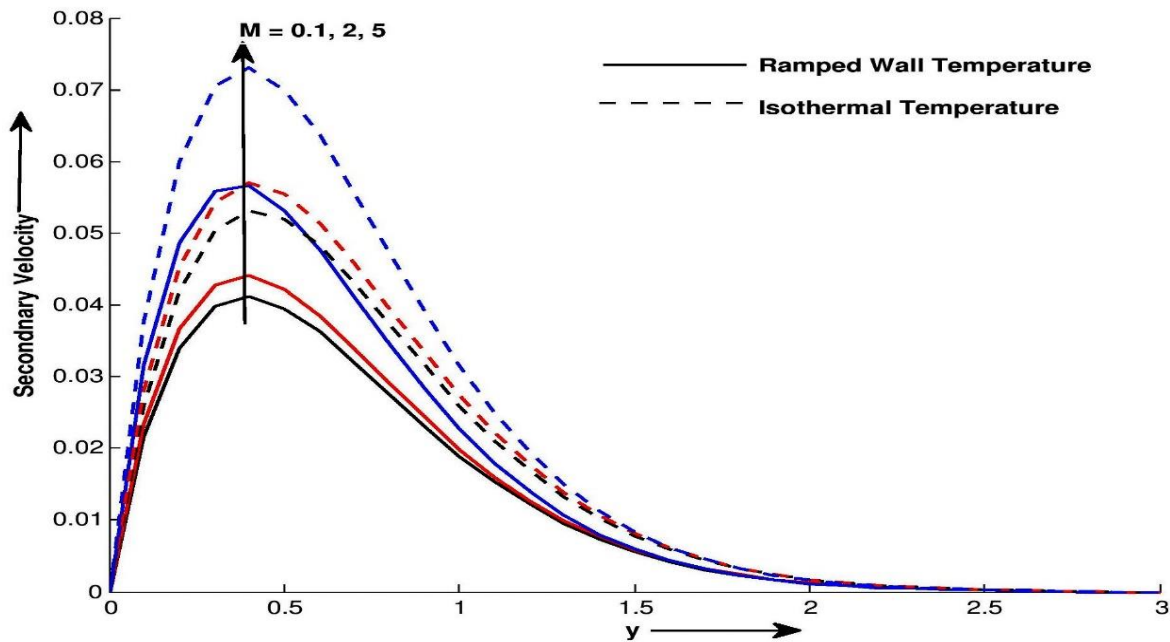


**Figure 7.1.7:** Secondary Velocity profile  $w$  for different values of  $y$  and  $M$  at  $\gamma = 1, m = 5, k = 0.5, k_1 = 2, Pr = 15, Sc = 6.2, H = 5, Gm = 2, Gr = 3, Nr = 3, Kr = 5, \omega_1 = \frac{\pi}{2}$  and  $t = 0.2$

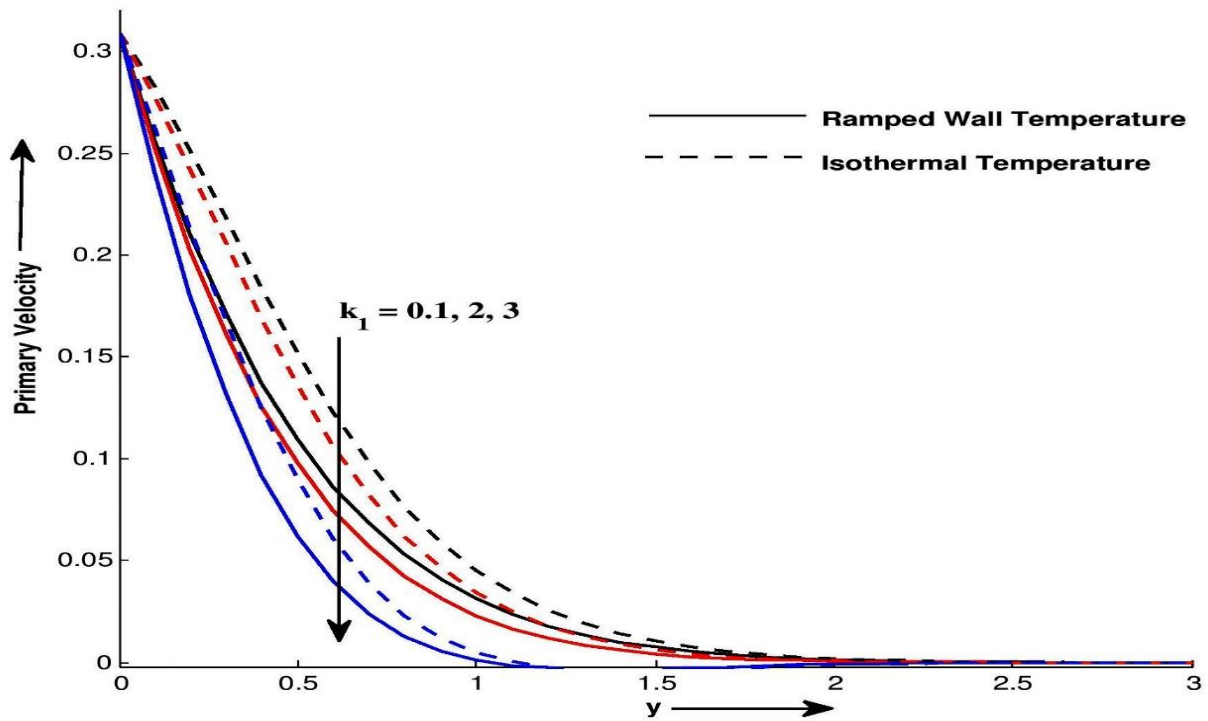


**Figure 7.1.8:** Primary Velocity profile  $u$  for different values of  $y$  and  $k_1$  at  $\gamma = 1, M = 1, k = 0.5, m = 5, Pr = 15, Sc = 6.2, H = 5, Gm = 2, Gr = 3, Nr = 3, Kr = 5, \omega_1 = \frac{\pi}{2}$  and  $t = 0.2$

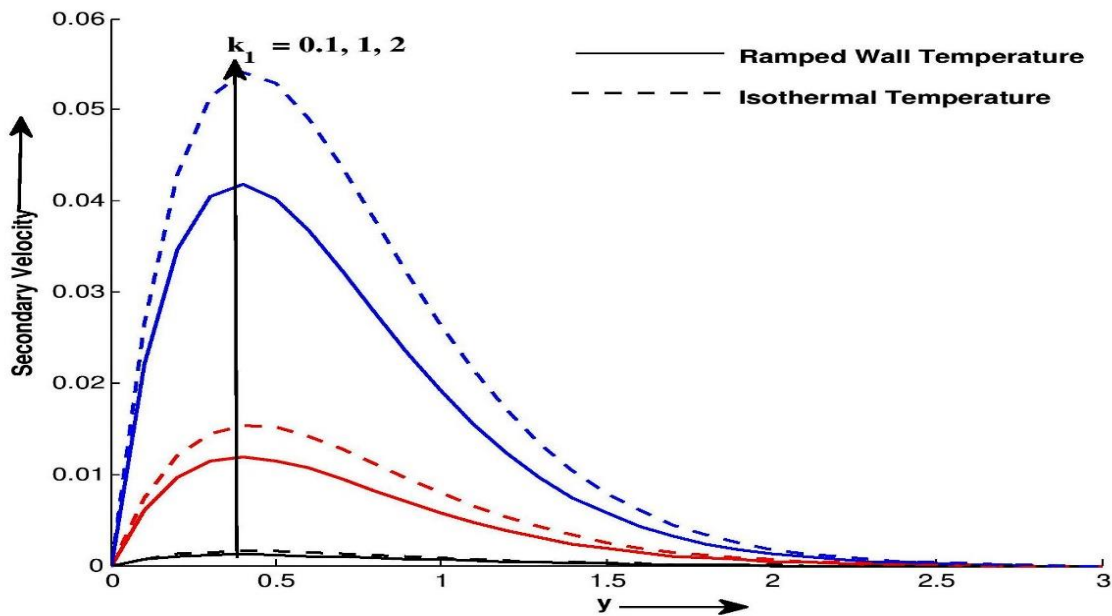


**Figure 7.1.9:** Secondary Velocity profile  $w$  for different values of  $y$  and  $k_1$  at  $\gamma = 1, M = 1, k = 0.5, m = 5, Pr = 15, Sc = 6.2, H = 5, Gm = 2, Gr = 3, Nr = 3, Kr = 5, \omega_1 = \frac{\pi}{2}$  and  $t = 0.2$

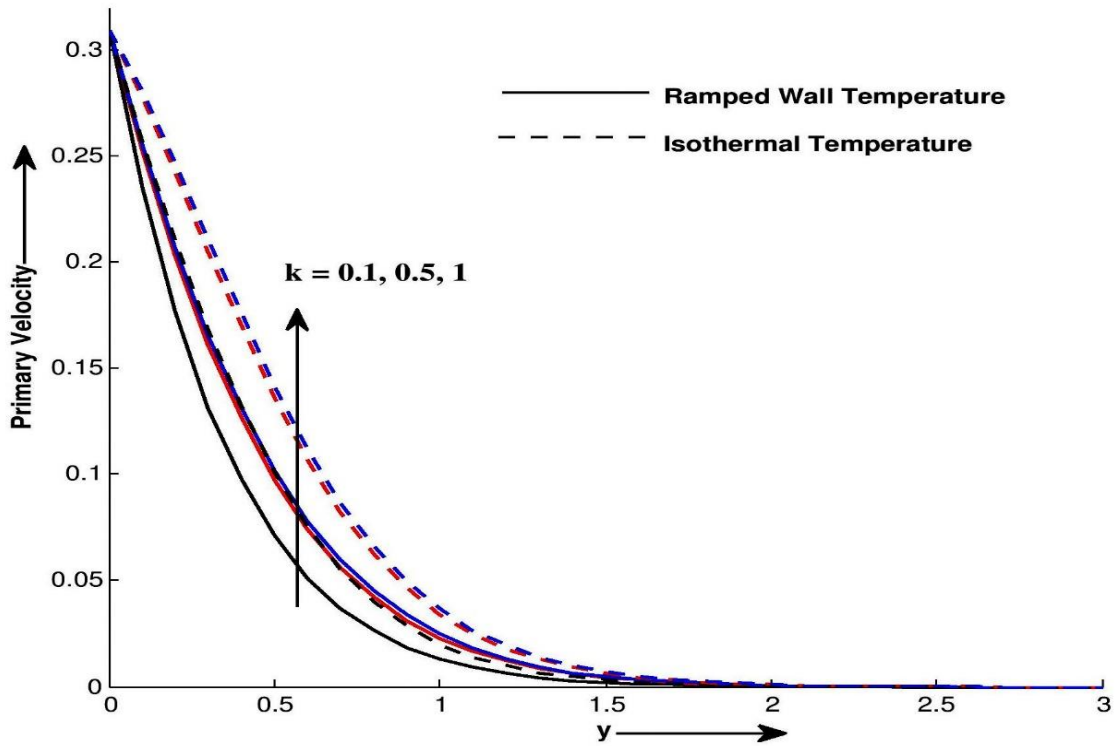


**Figure 7.1.10:** Primary Velocity profile  $u$  for different values of  $y$  and  $k$  at  $\gamma = 1, M = 1, m = 5, k_1 = 2, Pr = 15, Sc = 6.2, H = 5, Gm = 2, Gr = 3, Nr = 3, Kr = 5, \omega_1 = \frac{\pi}{2}$  and  $t = 0.2$

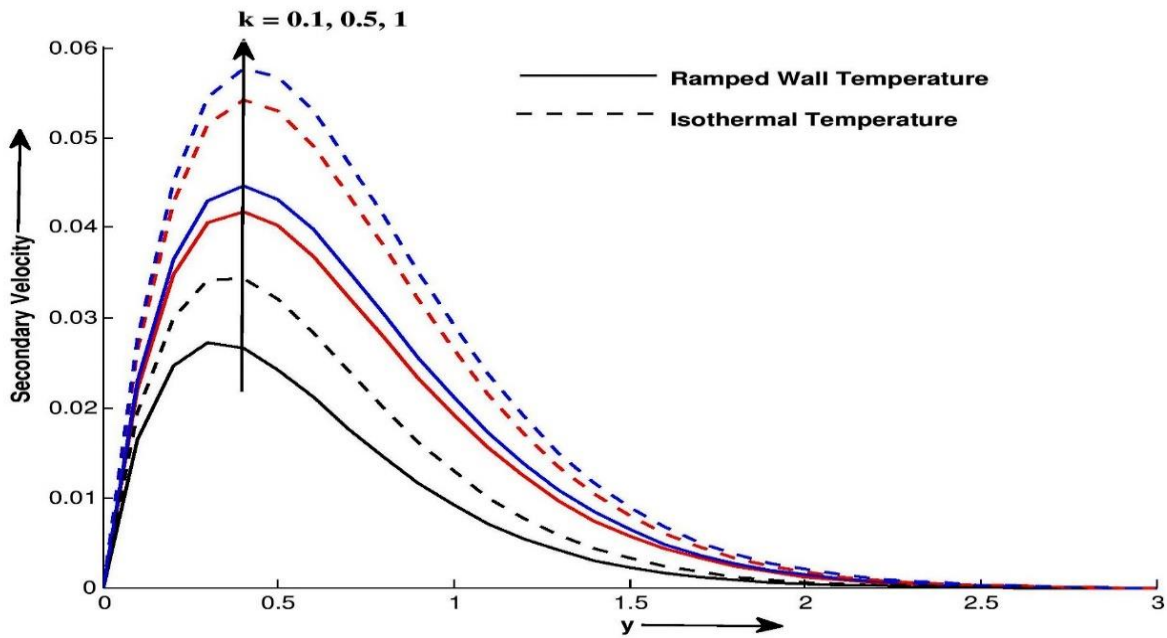


**Figure 7.1.11:** Secondary Velocity profile  $w$  for different values of  $y$  and  $k$  at  $\gamma = 1, M = 1, m = 5, k_1 = 2, Pr = 15, Sc = 6.2, H = 5, Gm = 2, Gr = 3, Nr = 3, Kr = 5, \omega_1 = \frac{\pi}{2}$  and  $t = 0.2$

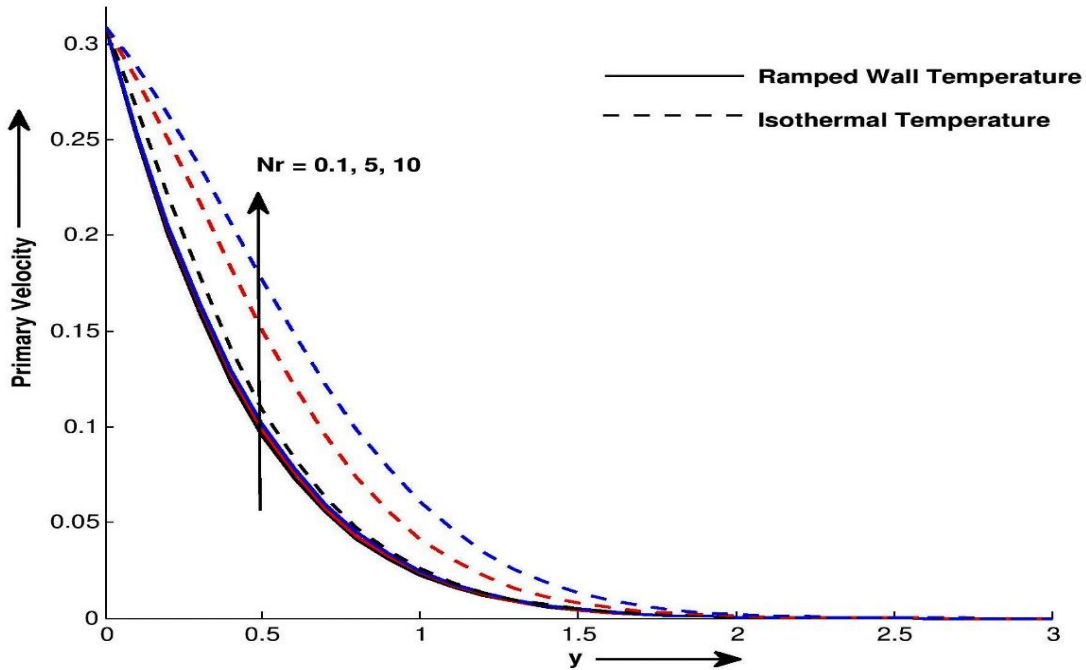


**Figure 7.1.12:** Primary Velocity profile  $u$  for different values of  $y$  and  $Nr$  at  $\gamma = 1, M = 1, k = 0.5, k_1 = 2, Pr = 15, Sc = 6.2, H = 5, Gm = 2, Gr = 3, m = 5, Kr = 5, \omega_1 = \frac{\pi}{2}$  and  $t = 0.2$

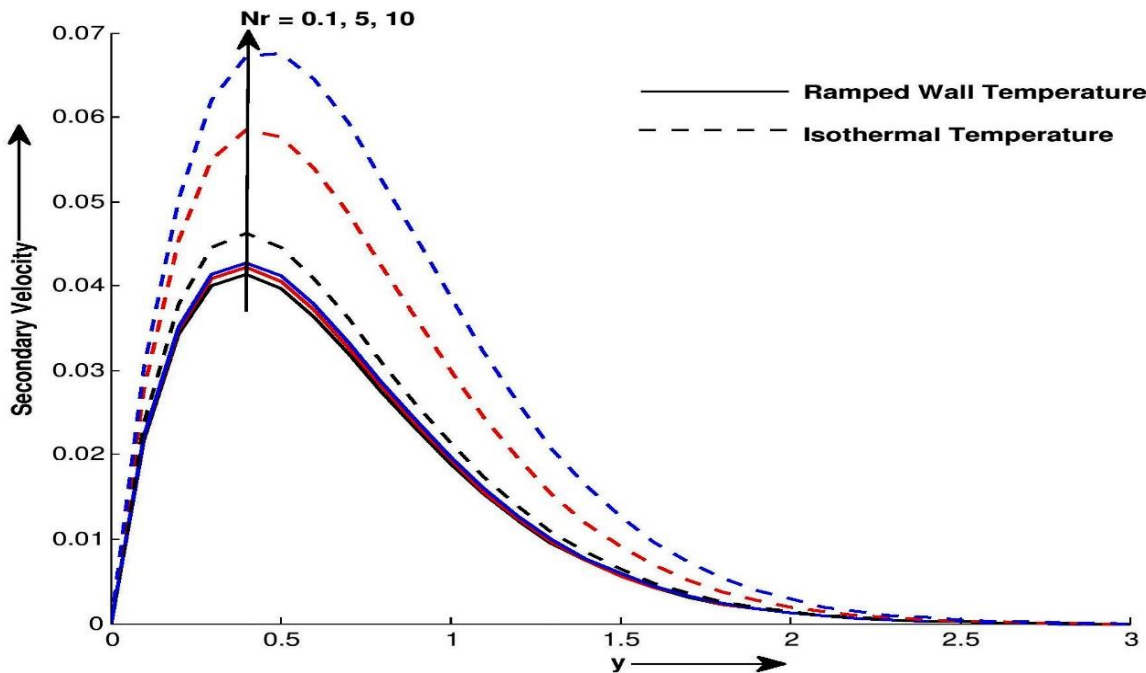


**Figure 7.1.13:** Secondary Velocity profile  $w$  for different values of  $y$  and  $Nr$  at  $\gamma = 1, M = 1, k = 0.5, k_1 = 2, Pr = 15, Sc = 6.2, H = 5, Gm = 2, Gr = 3, m = 5, Kr = 5, \omega_1 = \frac{\pi}{2}$  and  $t = 0.2$

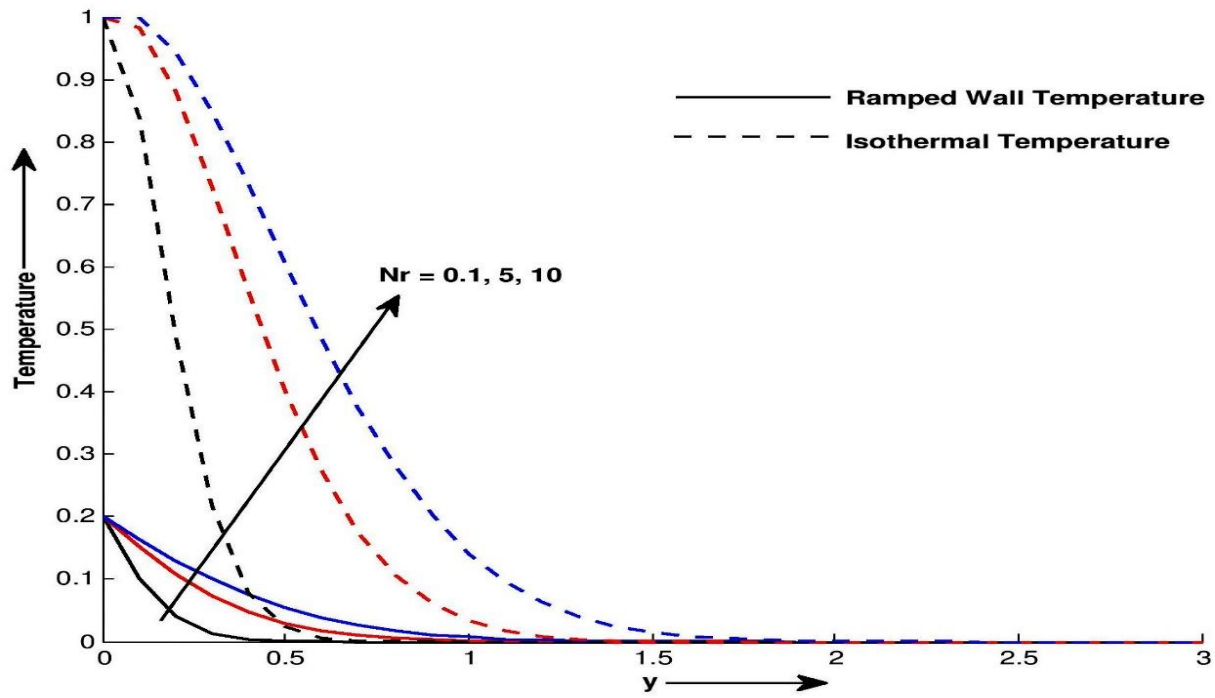


**Figure 7.1.14:** Temperature profile  $\theta$  for different values of  $y$  and  $Nr$  at  $Pr = 15, H = 5,$  and  $t = 0.2$

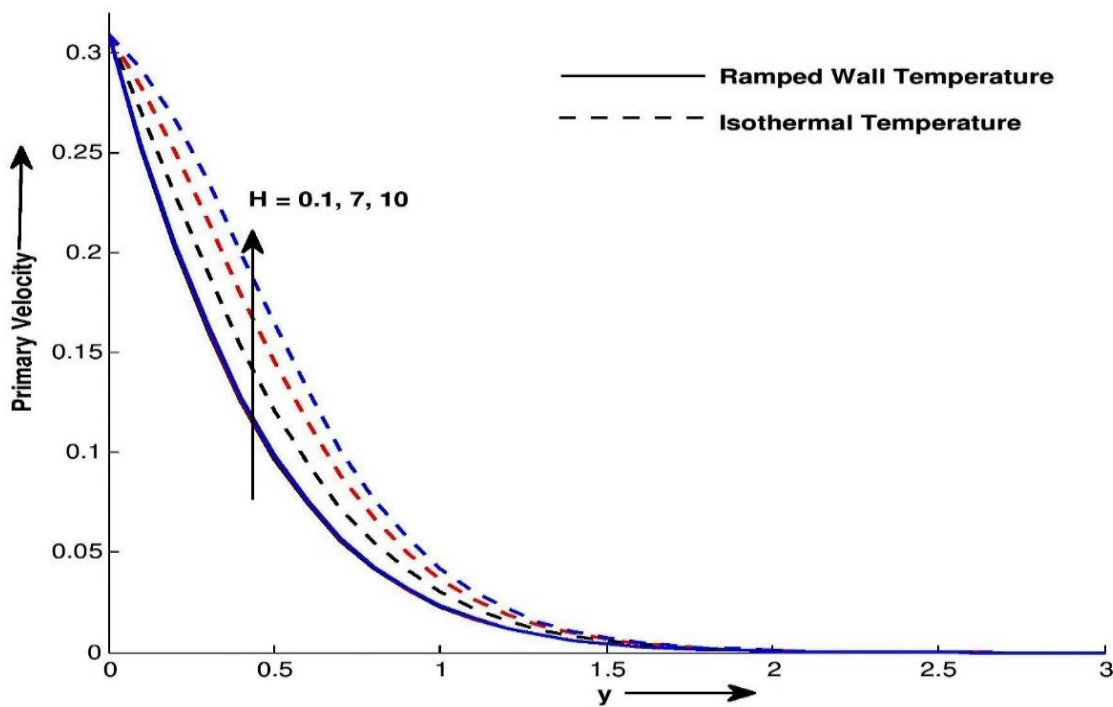


**Figure 7.1.15:** Primary Velocity profile  $u$  for different values of  $y$  and  $H$  at  $\gamma = 1, M = 1, k = 0.5, k_1 = 2, Pr = 15, Sc = 6.2, m = 5, Gm = 2, Gr = 3, Nr = 3, Kr = 5, \omega_1 = \frac{\pi}{2}$  and  $t = 0.2$

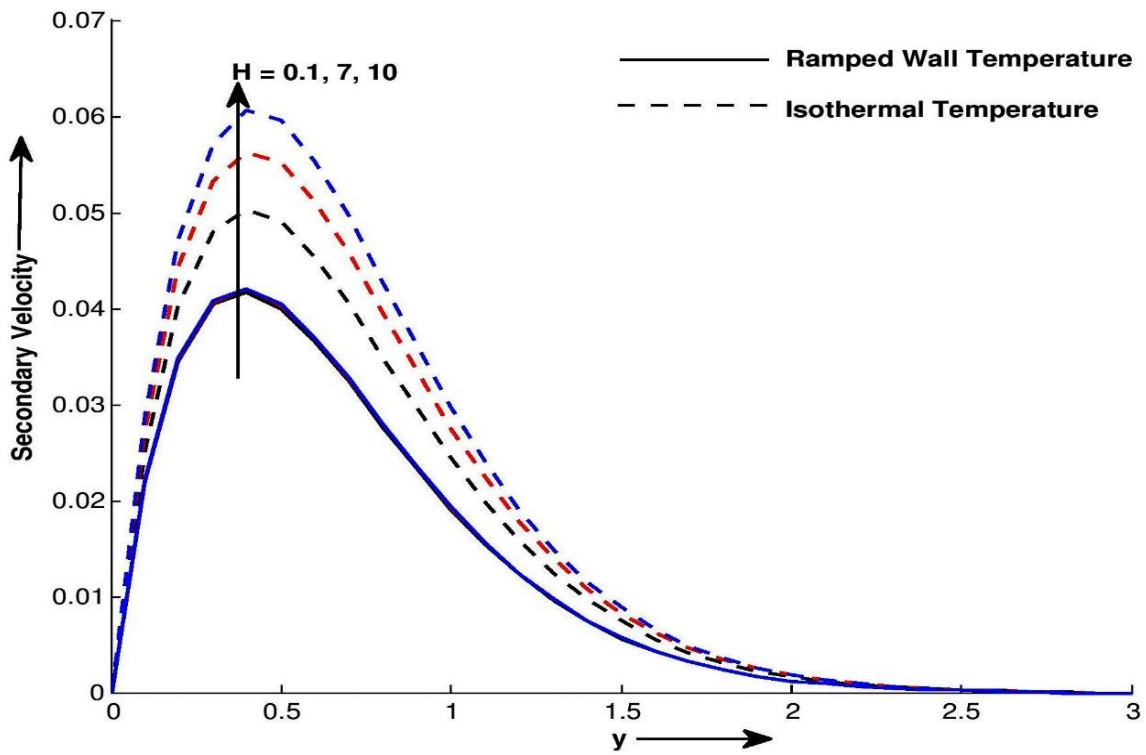


**Figure 7.1.16:** Secondary Velocity profile  $w$  for different values of  $y$  and  $H$  at  $\gamma = 1, M = 1, k = 0.5, k_1 = 2, Pr = 15, Sc = 6.2, m = 5, Gm = 2, Gr = 3, Nr = 3, Kr = 5, \omega_1 = \frac{\pi}{2}$  and  $t = 0.2$

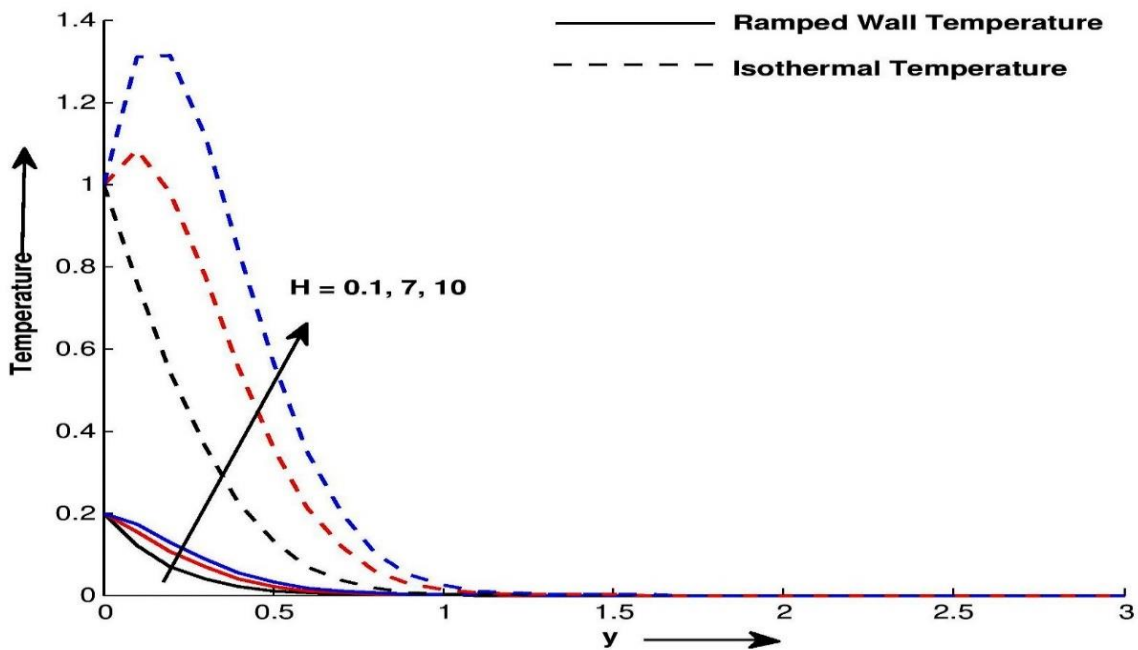


**Figure 7.1.17:** Temperature profile  $\theta$  for different values of  $y$  and  $H$  at  $Pr = 15, Nr = 3$  and  $t = 0.2$

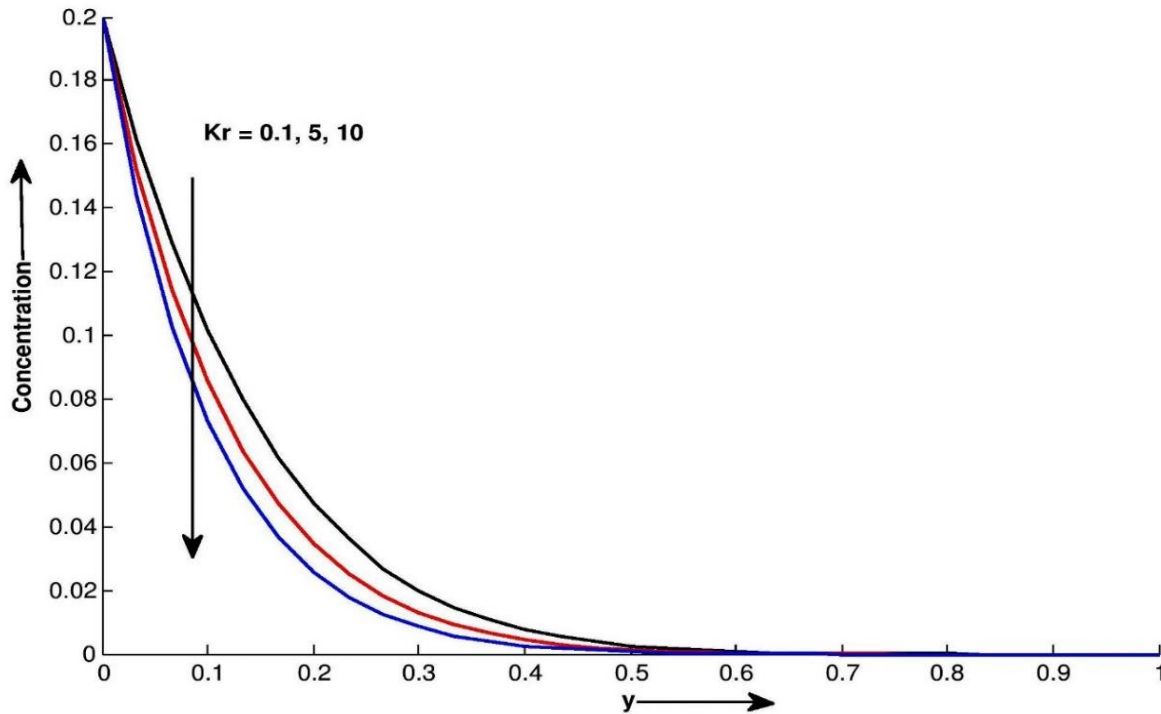


**Figure 7.1.18:** Concentration profile  $C$  for different values of  $y$  and  $Kr$  at  $Sc = 6.2$  and  $t = 0.2$

Figure 7.1.4 and Figure 7.1.5 show the effect of Casson fluid parameter  $\gamma$  on the primary and secondary velocities. It is observed that, primary velocity decreases with increase in Casson fluid throughout the boundary layer region, whereas secondary velocity initially increases then decrease with increase in  $\gamma$ . Figure 7.1.6 and Figure 7.1.7 illustrate primary velocity decreases with increases in  $M$  whereas secondary velocity increases with increases in  $M$ . This is due to Lorentz force effect on the boundary layer, which reduces motion of the fluid in  $x'$  direction. Figure 7.1.8 and Figure 7.1.9 demonstrate the influence of rotation  $k_1$  on the primary and secondary fluid velocities. It is evident from Figure 7.1.8 and Figure 7.1.9 that, for both thermal plates, rotation parameter  $k_1$  tends to decelerate fluid flow in primary flow directions, while rotation tends improve motion of the fluid flow in secondary flow direction. This is verified due to rotation, Coriolis force are created, tends to overturn fluid flow in the primary flow direction to induce secondary flow in the flow-field. Figure 7.1.10 and Figure 7.1.11 illustrate that permeability parameter  $k$  tends to improve motion of the fluid flow in both directions. Figure 7.1.12 to Figure 7.1.14 show effect of thermal radiation parameter  $Nr$  on primary velocity, secondary velocity and temperature profiles for both thermal plates. Physically, when the amount of heat generated through thermal radiation parameter increases, fluid elements

easily break then fluid velocities and temperature profiles will have increased. Figure 7.1.15 to Figure 7.1.17 show the effect of heat generation/absorption  $H$  on velocity and temperature profiles. These results are clearly supported from the physical point of view because heat source implies generation of heat from the surface of the region, which rises the temperature in the flow field. Therefore, velocities and temperature profiles increase with increase in  $H$ . Figure 7.1.18 shows effect of chemical reaction on concentration profile. It is seen that chemical reaction tends to reduce concentration throughout the flow field.

**Table 7.1.1:** Nusselt number variation

$Pr$	$H$	$Nr$	$t$	Nusselt number $Nu$ for Ramped Temperature	Nusselt number $Nu$ for isothermal Temperature
15	-1	5	0.4	1.2731	1.9399
16	-1	5	0.4	1.3149	2.0035
17	-1	5	0.4	1.3554	2.0651
15	-2	5	0.4	1.3416	2.1813
15	-3	5	0.4	1.4077	2.4094
15	-1	6	0.4	1.1787	1.7960
15	-1	7	0.4	1.1026	1.6800
15	-1	5	0.5	1.4620	1.8446
15	-1	5	0.6	1.6431	1.7810

**Table 7.1.2:** Sherwood number variation

$Sc$	$Kr$	$t$	Sherwood number $Sh$
0.66	2	0.4	0.7233
0.7	2	0.4	0.7449
1.0	2	0.4	0.8903
0.66	2.1	0.4	0.7299
0.66	2.2	0.4	0.7365
0.66	2	0.5	0.8454
0.66	2	0.6	0.9650

**Table 7.1.3:** Comparison of Nusselt number with Ref. [149] and Ref. [151]

$t$	$-H$	$Pr$	Nu for ramped temp. Ref [149]	Nu for ramped temp. Ref [151]	Nu for ramped temp.	Nu for isothermal temp. Ref [149]	Nu for isothermal temp. Ref [151]	Nu for isother mal temp.
0.3	1	0.71	0.57134752	0.571348	0.5713	1.11605411	1.11605	1.1161
0.5	1	0.71	0.77913255	0.779133	0.7791	0.98302070	0.983021	0.9830
0.7	1	0.71	0.96929143	0.969291	0.9693	0.92531051	0.925311	0.9253
0.7	1	0.71	0.96929143	0.969291	0.9693	0.92531051	0.925311	0.9253
0.7	3	0.71	1.26243402	1.26243	1.2624	1.47003548	1.47004	1.4700
0.7	5	0.71	1.50704023	1.50704	1.5070	1.88594507	1.88595	1.8859
0.7	1	0.50	0.81341130	-	0.8134	0.77650333	-	0.7765
0.7	1	0.71	0.96929143	-	0.9693	0.92531051	-	0.9253
0.7	1	7.00	3.04350641	-	3.0435	2.90540943	-	2.9054

Table (7.1.1) and Table (7.1.2) show variation of the Nusslet number and Sherwood number. It is depicted that, for both thermal conditions, temperature gradient increases with  $Pr, H$  and  $t$  whereas decreases with  $Nr$ . Table 7.1.2 shows concentration gradient at the surface increases with increase in  $Kr, Sc$  and  $t$ . Table 7.1.3 validates our results in terms of Nusselt number as it shows strong agreement with Seth et al. [149] and Nandkeolyar et al. [151]

#### 7.1.4 Conclusion

The most important concluding remarks can be summarized as follows:

- Hall current, permeability of porous medium, thermal radiation and heat generation tend to improve motion of the flow field in both directions  $x'$  and  $z'$  throughout the flow field.
- Thermal radiation and heat generation tend to increase heat transfer process.
- Chemical reaction has retarding effects on concentration profile.

## **7.2 SECTION II: SORET AND HALL EFFECTS ON MHD FLOW OF RADIATING AND CHEMICALLY REACTIVE CASSON FLUID PAST AN EXPONENTIALLY ACCELERATE MOVING VERTICAL PLATE WITH RAMPED WALL TEMPERATURE AND RAMPED SURFACE CONCENTRATION IN ROTATING SYSTEM**

In this section, thermo-diffusion, heat generation and Hall current effects on MHD flow of Casson fluid past an exponentially moving vertical plate through porous medium in rotating frame are considered with ramped boundary conditions. The governing dimensionless momentum, energy and concentration equation are convert in linear partial differential equations with imposed initial boundary conditions. To analyze effects of ramped boundary conditions, the said problem is also discussed for isothermal boundary conditions. For both boundary conditions, analytic expression for primary and secondary velocities, temperature and concentration profiles are obtained using Laplace transform technique. Exact expressions for shear stress, temperature gradient and concentration gradient are also derived with the help of velocity, temperature and concentration profiles.

### **7.2.1 Introduction of the Prblem**

Casson fluid is one of the time independent Non-newtonian fluids such as blood, plastic etc. So, application of this fluid is very important in real word problems. Thermo-diffusion effects was first introduced by Soret. Recently, thermo-diffusion effects on MHD Casson fluid flow discussed many researchers like, Sulochana et al. [38], Hayat et al. [123], Kataria and Patel [127]. On other hand, Singh and Kumar [161] discussed free convection flow past an exponentially accelerated vertical plate. Pramanik [31], Nadeem et al. [46] and Reddy et al. [111] studied mass and heat transfer effects on MHD flow of Casson fluid past an exponentially vertical plate.

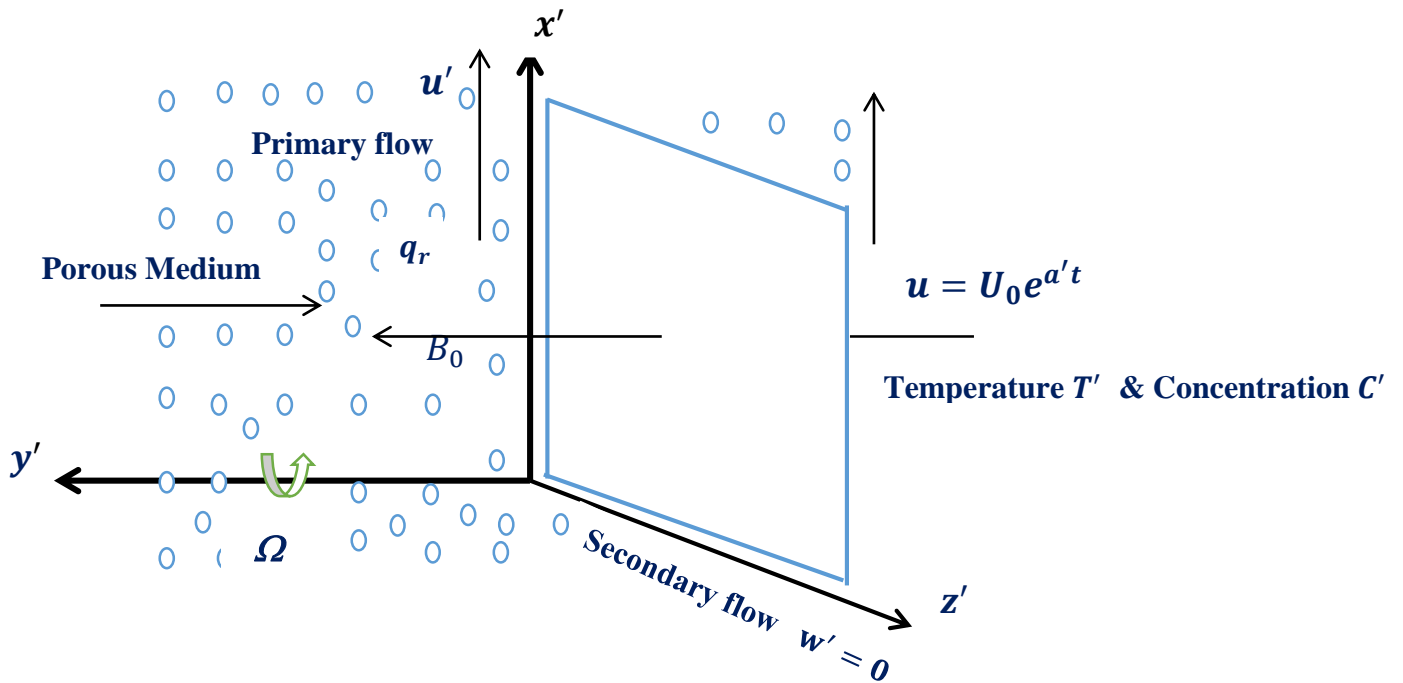
Today, study of many physical factors effects like, thermal radiation, chemical reaction, heat generation, thermo-diffusion and Hall current on MHD flow with Non-Newtonian fluid through porous medium in rotating system is attracted many researchers. Seth et al. [143-148] considered Hall effects on MHD flow in rotating system with different physical parameter.

### **7.2.2 Novelty of the Problem**

In previous section, Hall effects on MHD Casson fluid flow in rotating system with ramped boundary conditions are discussed without thermo-diffusion effects and not considering exponentially moving

plate. So, in this section, combine effects of thermo-diffusion and Hall current on flow of Casson fluid in presence of magnetic field in rotating frame are studied. To get perfect understanding of ramped wall temperature, the said problems is also discussed for both temperature and concentration boundary conditions are constant. For both boundary conditions, expressions for velocity in both directions, heat transfer and mass transfer are acquired using Laplace transform technique.

### 7.2.3 Mathematical Formulation of the Problem



$$T' = \begin{cases} T'_\infty + (T'_w - T'_\infty) t'/t_0 & \text{if } 0 < t' < t_0 \\ T'_w & \text{if } t' \geq t_0 \end{cases}, C' = \begin{cases} C'_\infty + (C'_w - C'_\infty) t'/t_0 & \text{if } 0 < t' < t_0 \\ C'_w & \text{if } t' \geq t_0 \end{cases}; y' = 0$$

Figure 7.2.1: Physical Sketch of the Model

As shown in Figure 7.2.1, coordinate system  $(x', y', z')$  is chosen such that  $x'$  – axis is taken along the vertical plate,  $y'$  – axis is taken normal to it and  $z'$  is perpendicular to  $x'y'$ . The fluid and plate rotate with angular velocity  $\Omega$  about  $y'$  – axis. The strength  $B_0$  is applied in  $y'$  – axis direction. Initially, at time  $t' \leq 0$ , fluid and the plate are at constant heat transfer  $T'_\infty$  and mass transfer  $C'_\infty$  respectively. At the time  $t' > 0$ , plate exponentially accelerated in  $x'$  – direction with primary velocity  $U_0 e^{a't}$ . Temperature of the wall is instantaneously raised and lowered to  $T'_\infty + (T'_w +$

$T'_\infty$ )  $t'/t_0$  when  $t' \leq t_0$  and  $T'_w$  when  $t' > t_0$  respectively which is there after maintained constant  $T'_w$  and the level of concentration at the surface of the plate is raised or lowered to  $C'_\infty + (C'_w + C'_\infty) t'/t_0$  when  $t' \leq t_0$  and  $C'_w$  when  $t' > t_0$  respectively which is there after maintained constant  $C'_w$ . It is assumed that the effects of viscous dissipation, induce magnetic and electrical field are negligible. Under above assumptions and taking into account the Boussinesq approximation governing equations are given below

$$\rho \frac{\partial u'}{\partial t'} + 2\Omega w' = \mu B \left(1 + \frac{1}{\gamma}\right) \frac{\partial^2 u'}{\partial y'^2} - \frac{\sigma B_0^2}{(1+m^2)} (u' + mw') - \frac{\mu B}{k'_1} u' + g\rho\beta'_T (T' - T'_\infty) + g\rho\beta'_C (C' - C'_\infty) \quad (7.2.1)$$

$$\rho \frac{\partial w'}{\partial t'} - 2\Omega u' = \mu B \left(1 + \frac{1}{\gamma}\right) \frac{\partial^2 w'}{\partial y'^2} - \frac{\sigma B_0^2}{(1+m^2)} (mu' - w') - \frac{\mu B}{k'_1} u' \quad (7.2.2)$$

$$\frac{\partial T'}{\partial t'} = \frac{k}{\rho c_p} \frac{\partial^2 T'}{\partial y'^2} - \frac{1}{\rho c_p} \frac{\partial q_r}{\partial y'} + \frac{Q_0}{\rho c_p} (T' - T'_\infty) \quad (7.2.3)$$

$$\frac{\partial C'}{\partial t'} = D_M \frac{\partial^2 C'}{\partial y'^2} + D_T \frac{\partial^2 T'}{\partial y'^2} - k'_2 (C' - C'_\infty) \quad (7.2.4)$$

with following initial and boundary conditions:

$$u' = 0, v' = 0 \quad T' = T'_\infty, C' = C'_\infty; \text{ as } y' \geq 0 \text{ and } t' \leq 0$$

$$u' = U_0 e^{a't}, w' = 0, T' = \begin{cases} T'_\infty + (T'_w - T'_\infty) t'/t_0 & \text{if } 0 < t' < t_0, \\ T'_w & \text{if } t' \geq t_0 \end{cases},$$

$$C' = \begin{cases} C'_\infty + (C'_w - C'_\infty) t'/t_0 & \text{if } 0 < t' < t_0; y' = 0, \\ C'_w & \text{if } t' \geq t_0 \end{cases}$$

$$u' \rightarrow 0, w' \rightarrow 0, T' \rightarrow T'_\infty, C' \rightarrow C'_\infty; \text{ as } y' \rightarrow \infty \text{ and } t' \geq 0 \quad (7.2.5)$$

Introducing the following dimensionless quantities;

$$y = \frac{y'}{U_0 t_0}, u = \frac{u'}{U_0}, t = \frac{t'}{t_0}, \theta = \frac{(T' - T'_\infty)}{(T'_w - T'_\infty)}, C = \frac{(C' - C'_\infty)}{(C'_w - C'_\infty)}, Gr = \frac{v g \beta'_T (T'_w - T'_\infty)}{U_0^3},$$

$$Gm = \frac{v g \beta'_C (C'_w - C'_\infty)}{U_0^3}, M = \frac{\sigma B_0^2 v}{\rho U_0^2}, P_r = \frac{\rho v c_p}{k}, Nr = \frac{16 a \sigma v^2 T'^3_\infty}{k U_0^2}, H = \frac{Q_0 v^2}{k U_0^2},$$

$$Kr = \frac{v k'_2}{U_0^2}, \alpha = \frac{\alpha_1}{\rho}, k_1 = \frac{v \phi}{k'_1}, Sr = \frac{D_T (T'_w - T'_\infty)}{v (C'_w - C'_\infty)}, Sc = \frac{v}{D_M}$$

$$\frac{\partial q_r}{\partial y'} = -4a\sigma (T'^4_\infty - T'^4), T'^4 \cong 4T'^3_\infty T' - 3T'^4_\infty$$

Using the substitution  $F = u + iw$ , equations 7.2.1 and 7.2.2 becomes;

$$\frac{\partial F}{\partial t} + \left( \frac{M^2(1-im)}{1+m^2} + \frac{1}{k_1} - 2ik^2 \right) F = \frac{\partial^2 F}{\partial y^2} + G_r \theta + G_m C \quad (7.2.6)$$

Using dimensionless quantities, equations 7.2.3 and 7.2.4 becomes;

$$\frac{\partial \theta}{\partial t} = \frac{(1+Nr)}{Pr} \frac{\partial^2 \theta}{\partial y^2} + \frac{H}{Pr} \theta \quad (7.2.7)$$

$$\frac{\partial C}{\partial t} = \frac{1}{Sc} \frac{\partial^2 C}{\partial y^2} + Sr \frac{\partial^2 \theta}{\partial y^2} - krC \quad (7.2.8)$$

with initial and boundary condition

$$F = \theta = C = 0, \quad y \geq 0, t \leq 0, F = e^{a't}, \quad \theta = \begin{cases} t, & 0 < t \leq 1 \\ 1 & t > 1 \end{cases},$$

$$C = \begin{cases} t, & 0 < t \leq 1 \\ 1 & t > 1 \end{cases} \quad \text{at } y = 0, t > 0$$

$$F \rightarrow 0, \theta \rightarrow 0, C \rightarrow 0 \quad \text{at } y \rightarrow \infty, t > 0 \quad (7.2.9)$$

## 7.2.4 Solution of the Problem

Analytical expression for Primary and Secondary velocities, temperature and concentration profiles are obtained from equations (7.2.6) to (7.2.8) with initial boundary condition (7.2.9) using the Laplace transform technique.

### 7.2.4.1 Solution of the problem for ramped temperature and ramped surface concentration

$$\theta(y, t) = f_7(y, t) - f_7(y, t - 1)H(t - 1), \quad (7.2.10)$$

$$C(y, t) = f_{11}(y, t) - f_{11}(y, t - 1)H(t - 1) - g_8(y, t) + g_8(y, t - 1)H(t - 1) + g_9(y, t) - g_9(y, t - 1)H(t - 1), \quad (7.2.11)$$

$$F(y, t) = g_1(y, t) + h_1(y, t) - h_1(y, t - 1)H(t - 1) \quad (7.2.12)$$

### 7.2.4.2 Solution of the problem for isothermal temperature and constant surface concentration

$$\theta(y, t) = f_6(y, t), \quad C(y, t) = f_{10}(y, t) - g_{10}(y, t) + g_{11}(y, t) \quad (7.2.13)$$

$$F(y, t) = g_1(y, t) + g_5(y, t) + g_6(y, t) + g_7(y, t) \quad (7.2.14)$$

$$C(y, t) = f_{10}(y, t) - g_{10}(y, t) + g_{11}(y, t) \quad (7.2.15)$$

Where

$$h_1(y, t) = g_2(y, t) - g_3(y, t) + g_4(y, t) \quad (7.2.16)$$

$$g_1(y, t) = \frac{e^{a't}}{2} \left[ e^{-y\sqrt{\frac{1}{a}(b+a')}} \operatorname{erfc} \left( \frac{y}{2\sqrt{at}} - \sqrt{(b+a')t} \right) + e^{y\sqrt{\frac{1}{a}(b+a')}} \operatorname{erfc} \left( \frac{y}{2\sqrt{at}} + \sqrt{(b+a')t} \right) \right] \quad (7.2.17)$$

$$g_2(y, t) = a_{30}f_1(y, t) + a_{31}f_2(y, t) + a_{32}f_3(y, t) + a_{33}f_4(y, t) + a_{34}f_5(y, t) \quad (7.2.18)$$

$$g_3(y, t) = a_{35}f_6(y, t) + a_{36}f_7(y, t) + a_{37}f_8(y, t) + a_{27}f_9(y, t) \quad (7.2.19)$$

$$g_4(y, t) = a_{38}f_{10}(y, t) + a_{39}f_{11}(y, t) + a_{40}f_{12}(y, t) + a_{23}f_{13}(y, t) \quad (7.2.20)$$

$$g_5(y, t) = a_{31}f_1(y, t) + a_{45}f_3(y, t) + a_{47}f_5(y, t) - a_{46}f_4(y, t) \quad (7.2.21)$$

$$g_6(y, t) = -a_{36}f_6(y, t) - a_{45}f_8(y, t) - a_{43}f_9(y, t) \quad (7.2.22)$$

$$g_7(y, t) = a_{39}f_{10}(y, t) + a_{41}f_{13}(y, t) + a_{46}f_{12}(y, t) \quad (7.2.23)$$

$$g_8(y, t) = a_{50}f_{10}(y, t) + a_{48}f_{11}(y, t) + a_{49}f_{13}(y, t) \quad (7.2.24)$$

$$g_9(y, t) = a_{50}f_6(y, t) + a_{48}f_7(y, t) + a_{49}f_9(y, t) \quad (7.2.25)$$

$$g_{10}(y, t) = a_{48}f_{10}(y, t) + a_{51}f_{13}(y, t) \quad (7.2.26)$$

$$g_{11}(y, t) = a_{48}f_6(y, t) + a_{51}f_9(y, t) \quad (7.2.27)$$

$$f_1(y, t) = \frac{1}{2} \left[ e^{-y\sqrt{\frac{b}{a}}} \operatorname{erfc} \left( \frac{y}{2\sqrt{at}} - \sqrt{bt} \right) + e^{y\sqrt{\frac{b}{a}}} \operatorname{erfc} \left( \frac{y}{2\sqrt{at}} + \sqrt{bt} \right) \right] \quad (7.2.28)$$

$$f_2(y, t) = \frac{1}{2} \left[ \left( t - \frac{y}{2\sqrt{ab}} \right) e^{-y\sqrt{\frac{b}{a}}} \operatorname{erfc} \left( \frac{y}{2\sqrt{at}} - \sqrt{bt} \right) + \left( t + \frac{y}{2\sqrt{ab}} \right) e^{y\sqrt{\frac{b}{a}}} \operatorname{erfc} \left( \frac{y}{2\sqrt{at}} + \sqrt{bt} \right) \right] \quad (7.2.29)$$

$$f_3(y, t) = \frac{e^{a_8t}}{2} \left[ e^{-y\sqrt{\frac{1}{a}(b+a_8)}} \operatorname{erfc} \left( \frac{y}{2\sqrt{at}} - \sqrt{(b+a_8)t} \right) + e^{y\sqrt{\frac{1}{a}(b+a_8)}} \operatorname{erfc} \left( \frac{y}{2\sqrt{at}} + \sqrt{(b+a_8)t} \right) \right] \quad (7.2.30)$$

$$f_4(y, t) = \frac{e^{-a_{12}t}}{2} \left[ e^{-y\sqrt{\frac{1}{a}(b-a_{12})}} \operatorname{erfc} \left( \frac{y}{2\sqrt{at}} - \sqrt{(b-a_{12})t} \right) + e^{y\sqrt{\frac{1}{a}(b-a_{12})}} \operatorname{erfc} \left( \frac{y}{2\sqrt{at}} + \sqrt{(b-a_{12})t} \right) \right] \quad (7.2.31)$$

$$f_5(y, t) = \frac{e^{a_4 t}}{2} \left[ e^{-y \sqrt{\frac{1}{a}(b+a_4)}} \operatorname{erfc} \left( \frac{y}{2\sqrt{a}t} - \sqrt{(b+a_4)t} \right) + e^{y \sqrt{\frac{1}{a}(b+a_4)}} \operatorname{erfc} \left( \frac{y}{2\sqrt{a}t} + \sqrt{(b+a_4)t} \right) \right] \quad (7.2.32)$$

$$f_6(y, t) = \frac{1}{2} \left[ e^{-y \sqrt{\frac{-d}{c}}} \operatorname{erfc} \left( \frac{y}{2\sqrt{ct}} - \sqrt{-dt} \right) + e^{y \sqrt{\frac{-d}{c}}} \operatorname{erfc} \left( \frac{y}{2\sqrt{ct}} + \sqrt{-dt} \right) \right] \quad (7.2.33)$$

$$f_7(y, t) = \frac{1}{2} \left[ \left( t - \frac{y}{2\sqrt{(-cd)}} \right) e^{-y \sqrt{\frac{-d}{c}}} \operatorname{erfc} \left( \frac{y}{2\sqrt{ct}} - \sqrt{-dt} \right) + \left( t + \frac{y}{2\sqrt{(-cd)}} \right) e^{y \sqrt{\frac{-d}{c}}} \operatorname{erfc} \left( \frac{y}{2\sqrt{ct}} + \sqrt{-dt} \right) \right] \quad (7.2.34)$$

$$f_8(y, t) = \frac{e^{a_8 t}}{2} \left[ e^{-y \sqrt{\frac{1}{c}(-d+a_8)}} \operatorname{erfc} \left( \frac{y}{2\sqrt{-c}t} - \sqrt{(-d+a_8)t} \right) + e^{y \sqrt{\frac{1}{c}(-d+a_8)}} \operatorname{erfc} \left( \frac{y}{2\sqrt{-c}t} + \sqrt{(-d+a_8)t} \right) \right] \quad (7.2.35)$$

$$f_9(y, t) = \frac{e^{a_4 t}}{2} \left[ e^{-y \sqrt{\frac{1}{c}(-d+a_4)}} \operatorname{erfc} \left( \frac{y}{2\sqrt{-c}t} - \sqrt{(-d+a_4)t} \right) + e^{y \sqrt{\frac{1}{c}(-d+a_4)}} \operatorname{erfc} \left( \frac{y}{2\sqrt{-c}t} + \sqrt{(-d+a_4)t} \right) \right] \quad (7.2.36)$$

$$f_{10}(y, t) = \frac{1}{2} \left[ e^{-y \sqrt{kr Sc}} \operatorname{erfc} \left( \frac{y \sqrt{Sc}}{2\sqrt{t}} - \sqrt{kr t} \right) + e^{y \sqrt{kr Sc}} \operatorname{erfc} \left( \frac{y \sqrt{Sc}}{2\sqrt{t}} + \sqrt{kr t} \right) \right] \quad (7.2.37)$$

$$f_{11}(y, t) = \frac{1}{2} \left[ \left( t - \frac{y \sqrt{Sc}}{2\sqrt{kr}} \right) e^{-y \sqrt{Sc kr}} \operatorname{erfc} \left( \frac{y \sqrt{Sc}}{2\sqrt{t}} - \sqrt{kr t} \right) + \left( t + \frac{y \sqrt{Sc}}{2\sqrt{kr}} \right) e^{y \sqrt{Sc kr}} \operatorname{erfc} \left( \frac{y \sqrt{Sc}}{2\sqrt{t}} + \sqrt{kr t} \right) \right] \quad (7.2.38)$$

$$f_{12}(y, t) = \frac{e^{-a_{12} t}}{2} \left[ e^{-y \sqrt{Sc(kr-a_{12})}} \operatorname{erfc} \left( \frac{y \sqrt{Sc}}{2\sqrt{t}} - \sqrt{(kr-a_{12})t} \right) + e^{y \sqrt{Sc(kr-a_{12})}} \operatorname{erfc} \left( \frac{y \sqrt{Sc}}{2\sqrt{t}} + \sqrt{(kr-a_{12})t} \right) \right] \quad (7.2.39)$$

$$f_{13}(y, t) = \frac{e^{a_4 t}}{2} \left[ e^{-y \sqrt{Sc(kr+a_4)}} \operatorname{erfc} \left( \frac{y \sqrt{Sc}}{2\sqrt{t}} - \sqrt{(kr+a_4)t} \right) + e^{y \sqrt{Sc(kr+a_4)}} \operatorname{erfc} \left( \frac{y \sqrt{Sc}}{2\sqrt{t}} + \sqrt{(kr+a_4)t} \right) \right] \quad (7.2.40)$$

**7.2.4.3 Nusselt number**

Expressions of Nusselt number  $Nu$  can be written as

$$Nu = \left( \frac{\partial \theta}{\partial y} \right)_{y=0} \quad (7.2.41)$$

For ramped wall temperature and ramped surface concentration

$$Nu = I_7(t) - I_7(t - 1)H(t - 1) \quad (7.2.42)$$

For isothermal temperature and ramped surface concentration

$$Nu = I_6(t) \quad (7.2.43)$$

**7.2.4.4 Sherwood number**

Expressions of Sherwood number  $Sh$  as

$$Sh = \left( \frac{\partial C}{\partial y} \right)_{y=0} \quad (7.2.44)$$

For ramped wall temperature and ramped surface concentration

$$Sh = I_{11}(t) - I_{11}(t - 1)H(t - 1) - I_{21}(t) + I_{21}(t - 1)H(t - 1) + I_{22}(t) - I_{22}(t - 1)H(t - 1) \quad (7.2.45)$$

For isothermal temperature and ramped surface concentration

$$Sh = I_{10}(t) - I_{23}(t) + I_{24}(t) \quad (7.2.46)$$

**7.2.4.5 Skin friction**

Expressions of skin-friction as

$$\tau^*(y, t) = -\mu_B \left( 1 + \frac{1}{\gamma} \right) \tau \quad (7.2.47)$$

$$\text{Where } \tau = \left. \frac{\partial u}{\partial y} \right|_{y=0} \quad (7.2.48)$$

For ramped wall temperature and ramped surface concentration

$$\tau = I_{14}(t) + I_{25}(t) - I_{25}(t - 1)H(t - 1) \quad (7.2.49)$$

For isothermal temperature and ramped surface concentration

$$\tau = I_{14}(t) + I_{18}(t) + I_{19}(t) + I_{20}(t) \quad (7.2.50)$$

Where

$$I_{25}(t) = I_{15}(t) - I_{16}(t) + I_{17}(t) \quad (7.2.51)$$

$$I_{24}(t) = a_{48}I_6(t) + a_{51}I_9(t) \quad (7.2.52)$$

$$I_{23}(t) = a_{48}I_{10}(t) + a_{51}I_{13}(t) \quad (7.2.53)$$

$$I_{22}(t) = a_{50}I_6(t) + a_{48}I_7(t) + a_{49}I_9(t) \quad (7.2.54)$$

$$I_{21}(t) = a_{50}I_{10}(t) + a_{48}I_{11}(t) + a_{49}I_{13}(t) \quad (7.2.55)$$

$$I_{20}(t) = a_{39}I_{10}(t) + a_{41}I_{13}(t) + a_{46}I_{12}(t) \quad (7.2.56)$$

$$I_{19}(t) = -a_{36}I_6(t) - a_{45}I_8(t) - a_{43}I_9(t) \quad (7.2.57)$$

$$I_{18}(t) = a_{31}I_1(t) + a_{45}I_3(t) - a_{46}I_4(t) + a_{47}I_5(t) \quad (7.2.58)$$

$$I_{17}(t) = a_{38}I_{10}(t) + a_{39}I_{11}(t) + a_{40}I_{12}(t) + a_{23}I_{13}(t) \quad (7.2.59)$$

$$I_{16}(t) = a_{35}I_6(t) + a_{36}I_7(t) + a_{37}I_8(t) + a_{27}I_9(t) \quad (7.2.60)$$

$$I_{15}(t) = a_{30}I_1(t) + a_{31}I_2(t) + a_{32}I_3(t) + a_{33}I_4(t) + a_{34}I_5(t) \quad (7.2.61)$$

$$I_{14}(t) = e^{a't} \sqrt{\frac{b+a'}{a}} \operatorname{erf}\left(\sqrt{(b+a')t}\right) + \frac{e^{-bt}}{\sqrt{\pi at}} \quad (7.2.62)$$

$$I_{13}(t) = -e^{a_4 t} \sqrt{Sc(Kr + a_4)} \operatorname{erf}\left(\sqrt{(Kr + a_4)t}\right) + \sqrt{\frac{Sc}{\pi t}} e^{-Kr t} \quad (7.2.63)$$

$$I_{12}(t) = -e^{-a_{12} t} \sqrt{Sc(Kr - a_{12})} \operatorname{erf}\left(\sqrt{(Kr - a_{12})t}\right) + \sqrt{\frac{Sc}{\pi t}} e^{-Kr t} \quad (7.2.64)$$

$$I_{11}(t) = -\sqrt{\frac{Sc}{4kr}} \operatorname{erf}(\sqrt{kr t}) - t\sqrt{Sc kr} \operatorname{erf}(\sqrt{kr t}) + \sqrt{\frac{t Sc}{\pi}} e^{-kr t} \quad (7.2.65)$$

$$I_{10}(t) = -\sqrt{kr Sc} \operatorname{erf}(\sqrt{kr t}) + \sqrt{\frac{Sc}{\pi t}} e^{-kr t} \quad (7.2.66)$$

$$I_9(t) = e^{a_4 t} \sqrt{\frac{-d+a_4}{c}} \operatorname{erf}\left(\sqrt{(-d + a_4)t}\right) + \frac{e^{dt}}{\sqrt{\pi ct}} \quad (7.2.67)$$

$$I_8(t) = e^{a_8 t} \sqrt{\frac{-d+a_8}{c}} \operatorname{erf}(\sqrt{(-d+a_8)t}) + \frac{e^{dt}}{\sqrt{\pi ct}} \quad (7.2.68)$$

$$I_7(t) = -\frac{1}{\sqrt{-4cd}} \operatorname{erf}(\sqrt{-dt}) - t \sqrt{\frac{-d}{c}} \operatorname{erf}(\sqrt{-dt}) + \frac{t e^{dt}}{\sqrt{\pi ct}} \quad (7.2.69)$$

$$I_6(t) = -\sqrt{\frac{-d}{c}} \operatorname{erf}(\sqrt{-dt}) + \frac{e^{dt}}{\sqrt{\pi ct}} \quad (7.2.70)$$

$$I_5(t) = e^{a_4 t} \sqrt{\frac{b+a_4}{a}} \operatorname{erf}(\sqrt{(b+a_4)t}) + \frac{e^{-bt}}{\sqrt{\pi at}} \quad (7.2.71)$$

$$I_4(t) = e^{-a_{12} t} \sqrt{\frac{b-a_{12}}{a}} \operatorname{erf}(\sqrt{(b-a_{12})t}) + \frac{e^{-bt}}{\sqrt{\pi at}} \quad (7.2.72)$$

$$I_3(t) = e^{a_8 t} \sqrt{\frac{b+a_8}{a}} \operatorname{erf}(\sqrt{(b+a_8)t}) + \frac{e^{-bt}}{\sqrt{\pi at}} \quad (7.2.73)$$

$$I_2(t) = -\frac{1}{\sqrt{4ab}} \operatorname{erf}(\sqrt{bt}) - t \sqrt{\frac{b}{a}} \operatorname{erf}(\sqrt{bt}) + \frac{t e^{-bt}}{\sqrt{\pi at}} \quad (7.2.74)$$

$$I_1(t) = -\sqrt{\frac{b}{a}} \operatorname{erf}(\sqrt{bt}) + \frac{e^{-bt}}{\sqrt{\pi at}} \quad (7.2.75)$$

### 7.2.5 Result and Discussion

The primary velocity, secondary velocity, temperature and concentration profiles for several values of different physical parameters are shown in Figures (7.2.2) to (7.2.23). It is revealed from Figure 7.2.2 to Figure 7.2.17 that, for both thermal plates, primary velocity, secondary velocity, temperature and concentration profiles attain a distinctive maximum value near surface of the plate and then decrease appropriately on increasing boundary layer coordinate  $y$  to approach free stream value. Figure 7.2.2 to Figure 7.2.3 show the effect of Hall current  $m$  on primary and secondary fluid velocities for both thermal plates. It is seen that, Hall current tends to improve motion of the fluid in both directions  $x'$  and  $z'$  throughout the boundary layer region. Physically, Hall current tends to induce Secondary flow in the flow field, due to this effect and observations from both figures, It is concluded that motion of fluid in  $z'$  – direction is more than that  $x'$  – direction. Figure 7.2.4 and Figure 7.2.5 indicate Primary velocity decreases with increase in Casson fluid  $\gamma$  throughout the

boundary layer region, whereas Secondary velocity initially increases then decrease with increase in  $y$ .

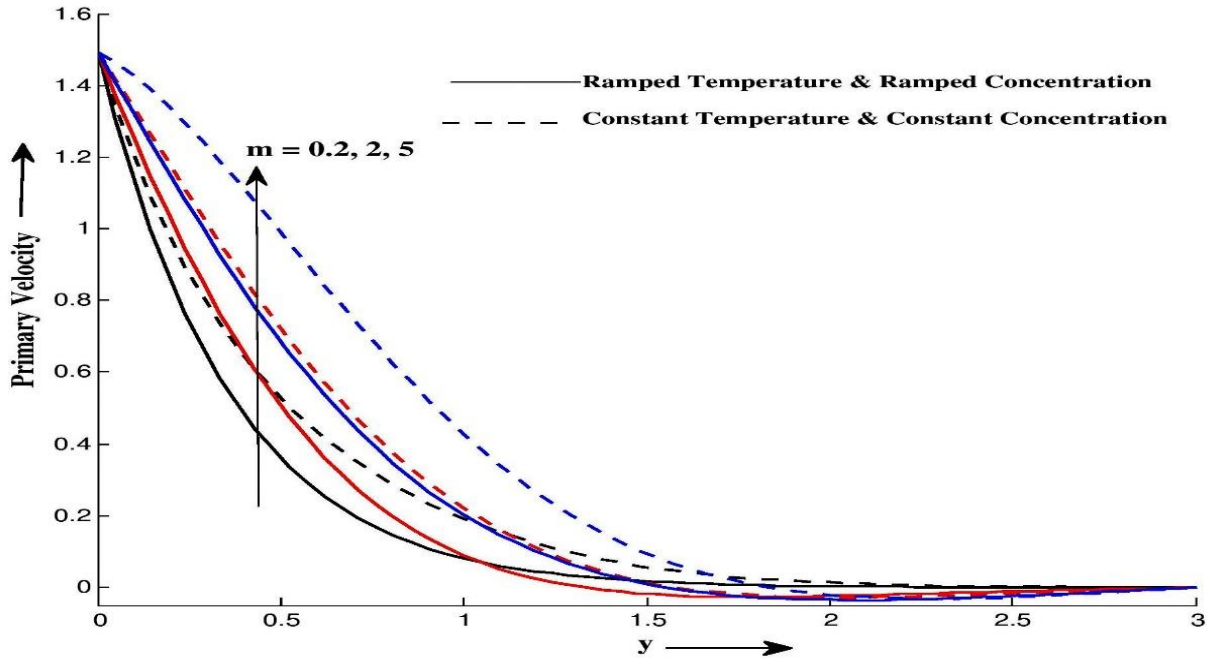


**Figure 7.2.2:** Primary Velocity  $u$  for different values of  $y$  and  $m$  at  $\gamma = 0.5, M = 5, k_1 = 1.5, k = 0.8, Pr = 7, Sc = 6.2, H = 5, Gm = 10, Gr = 5, Nr = 5, Sr = 3, Kr = 5$  and  $t = 0.4$

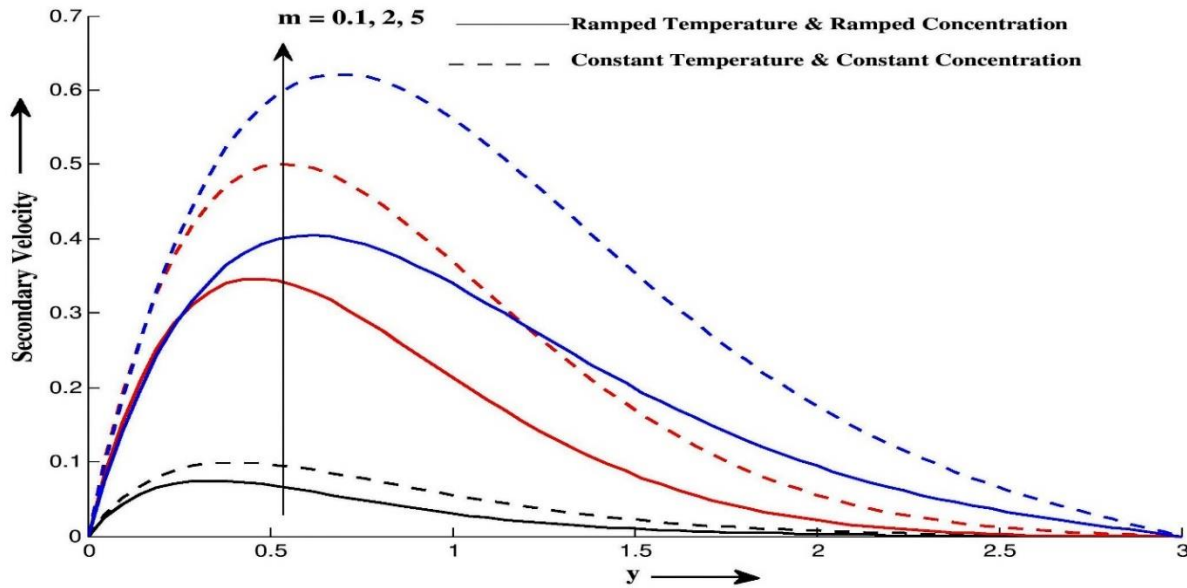


**Figure 7.2.3:** Secondary Velocity  $w$  for different values of  $y$  and  $m$  at  $\gamma = 0.5, M = 5, k_1 = 1.5, k = 0.8, Pr = 7, Sc = 6.2, H = 5, Gm = 10, Gr = 5, Nr = 5, Sr = 3, Kr = 5$  and  $t = 0.4$

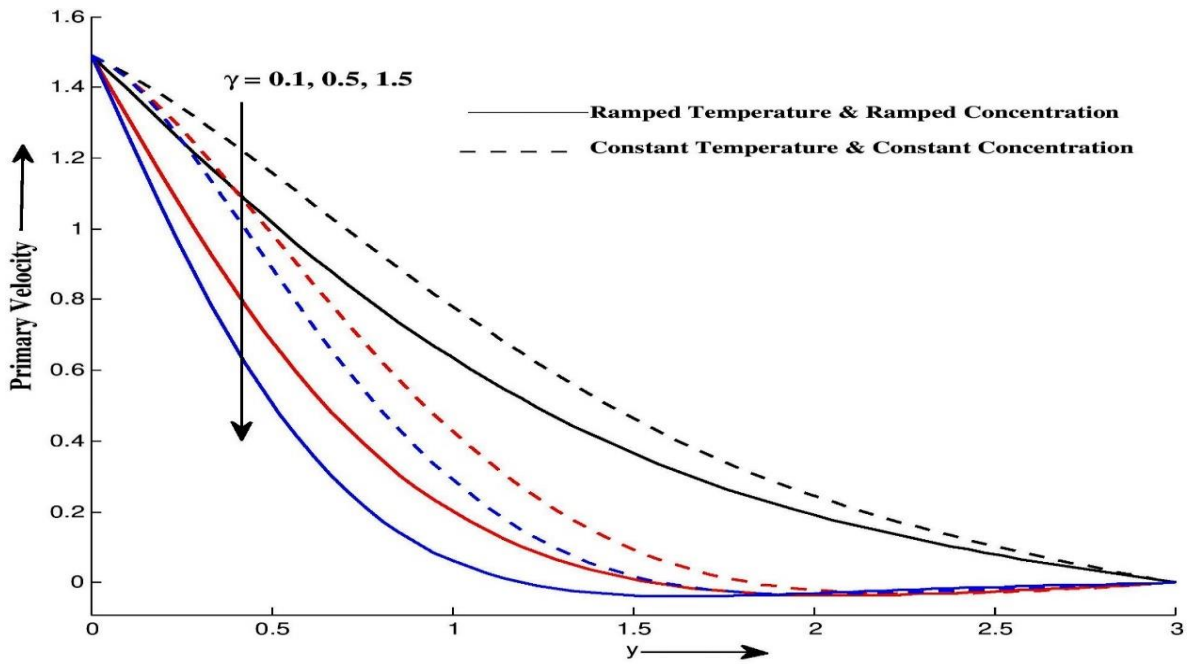


**Figure 7.2.4:** Primary Velocity  $u$  for different values of  $y$  and  $\gamma$  at  $m = 5, M = 5, k_1 = 1.5, k = 0.8, Pr = 7, Sc = 6.2, H = 5, Gm = 10, Gr = 5, Nr = 5, Sr = 3, Kr = 5$  and  $t = 0.4$

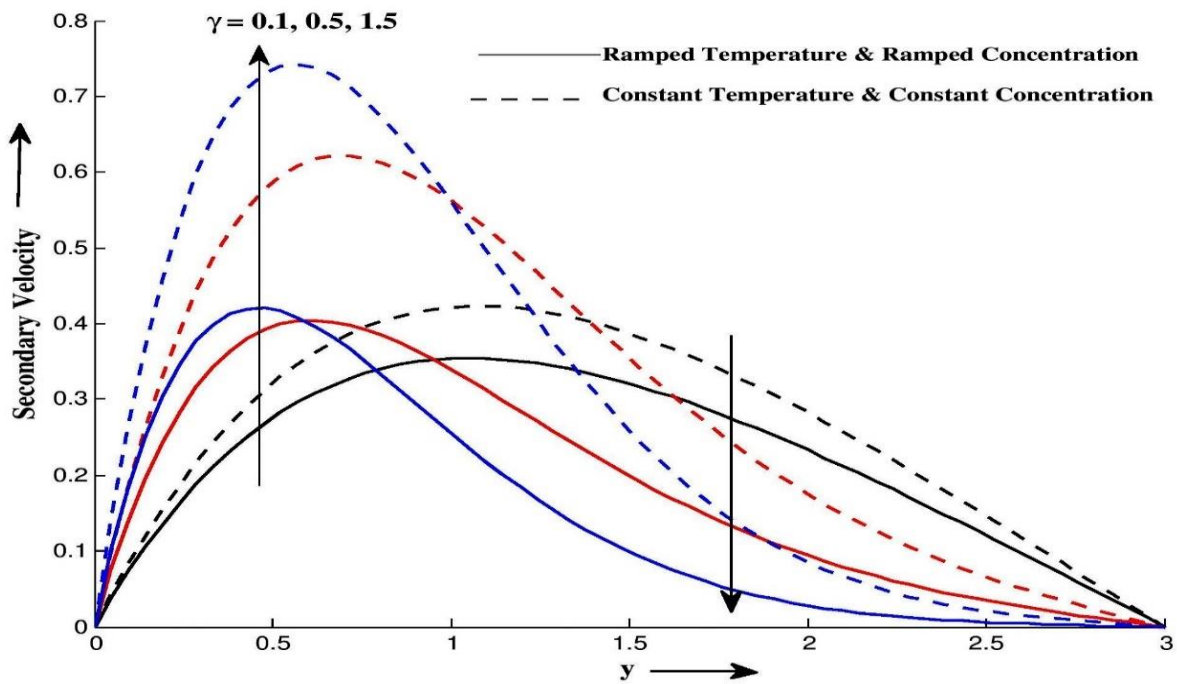


**Figure 7.2.5:** Secondary Velocity  $w$  for different values of  $y$  and  $\gamma$  at  $m = 5, M = 5, k_1 = 1.5, k = 0.8, Pr = 7, Sc = 6.2, H = 5, Gm = 10, Gr = 5, Nr = 5, Sr = 3, Kr = 5$  and  $t = 0.4$

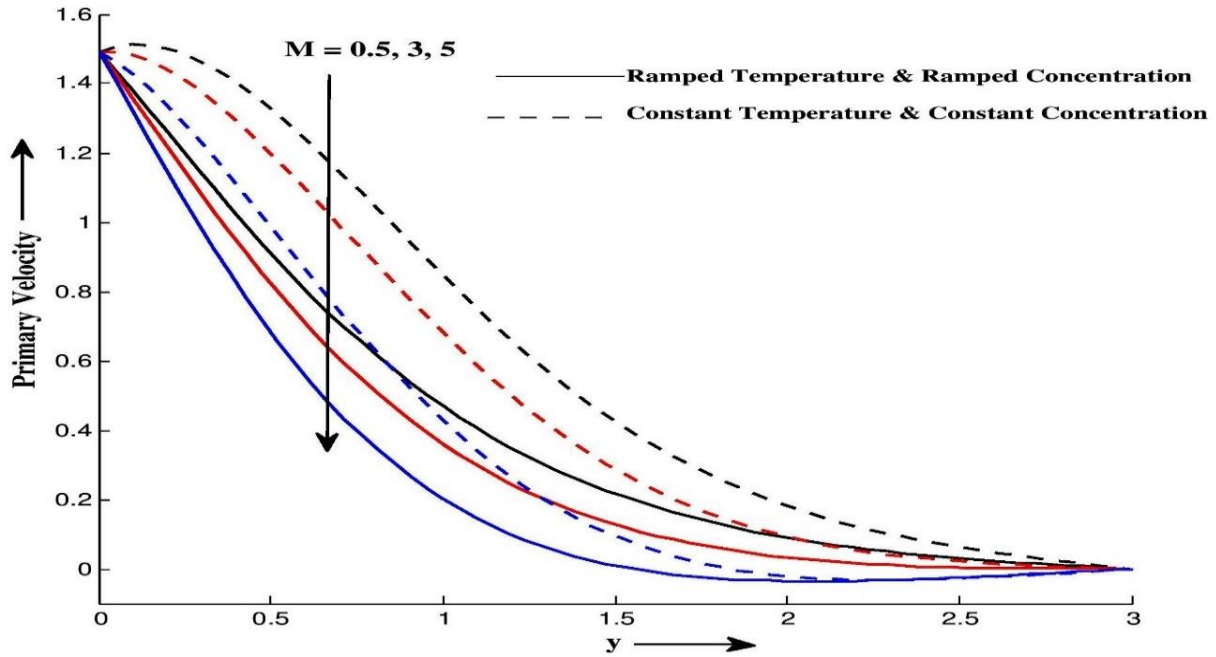


**Figure 7.2.6:** Primary Velocity  $u$  for different values of  $y$  and  $M$  at  $\gamma = 0.5, m = 5, k_1 = 1.5, k = 0.8, Pr = 7, Sc = 6.2, H = 5, Gm = 10, Gr = 5, Nr = 5, Sr = 3, Kr = 5$  and  $t = 0.4$

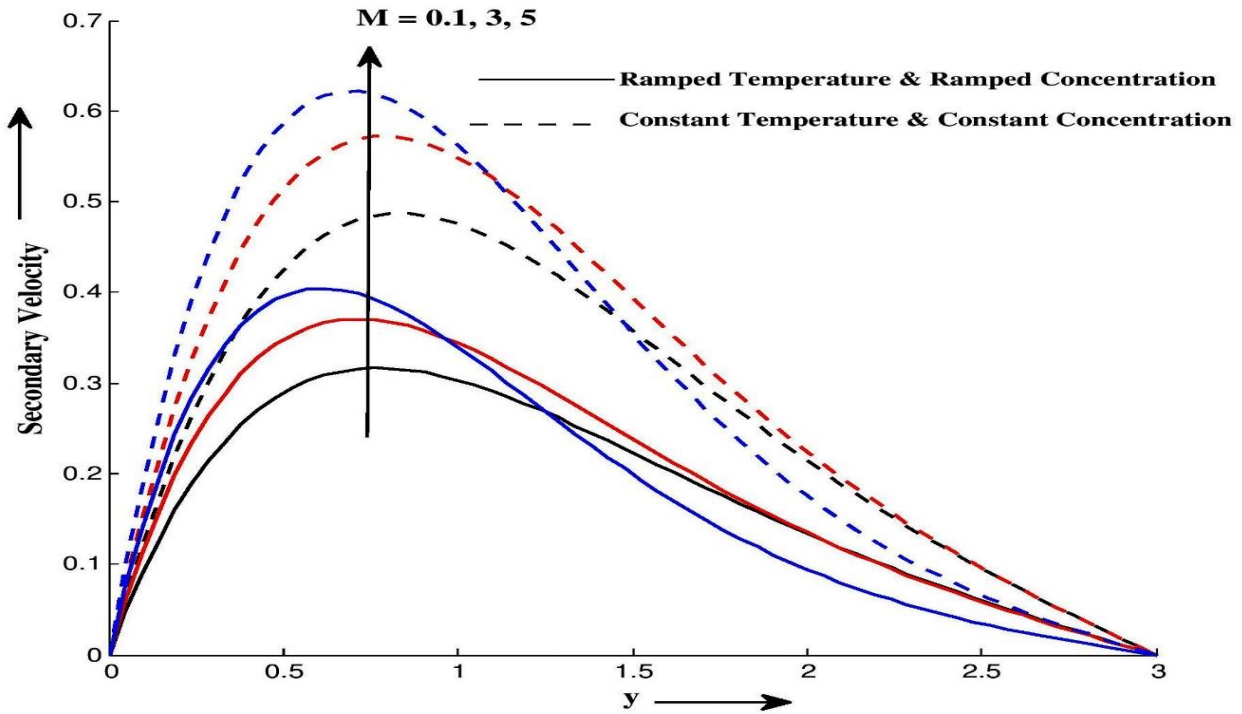


**Figure 7.2.7:** Secondary Velocity  $w$  for different values of  $y$  and  $M$  at  $\gamma = 0.5, M = 5, k_1 = 1.5, k = 0.8, Pr = 7, Sc = 6.2, H = 5, Gm = 10, Gr = 5, Nr = 5, Sr = 3, Kr = 5$  and  $t = 0.4$

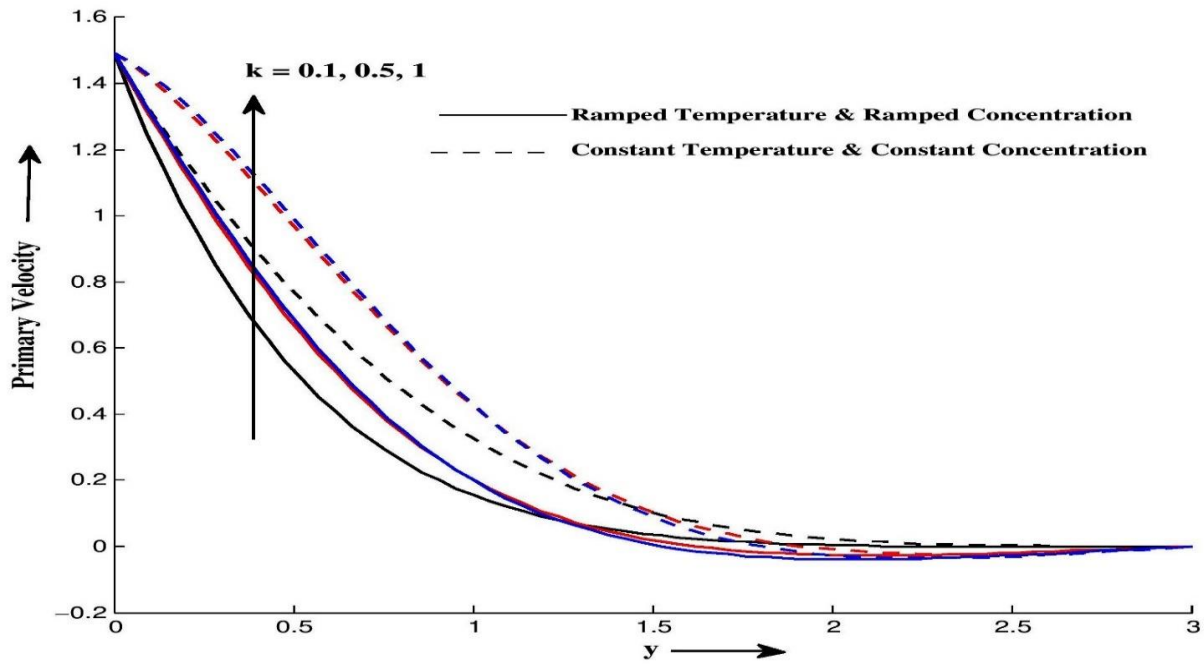


**Figure 7.2.8:** Primary Velocity  $u$  for different values of  $y$  and  $k$  at  $\gamma = 0.5, M = 5, k_1 = 1.5, m = 5, Pr = 7, Sc = 6.2, H = 5, Gm = 10, Gr = 5, Nr = 5, Sr = 3, Kr = 5$  and  $t = 0.4$

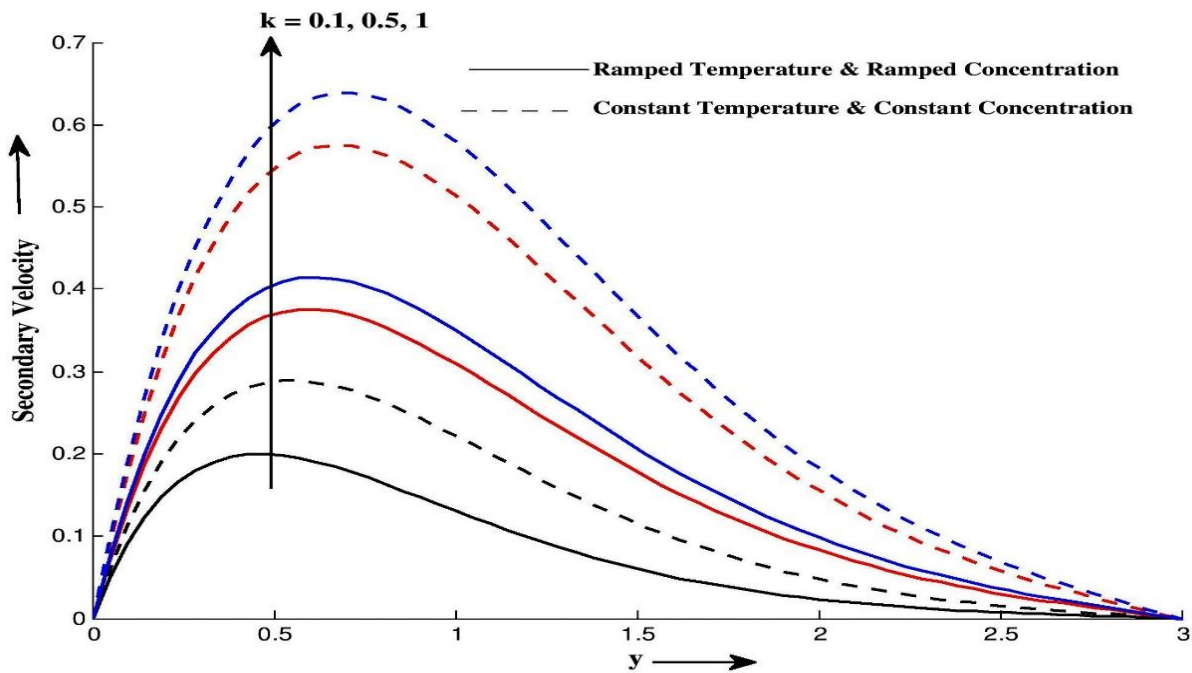


**Figure 7.2.9:** Secondary Velocity  $w$  for different values of  $y$  and  $k$  at  $\gamma = 0.5, M = 5, k_1 = 1.5, m = 5, Pr = 7, Sc = 6.2, H = 5, Gm = 10, Gr = 5, Nr = 5, Sr = 3, Kr = 5$  and  $t = 0.4$

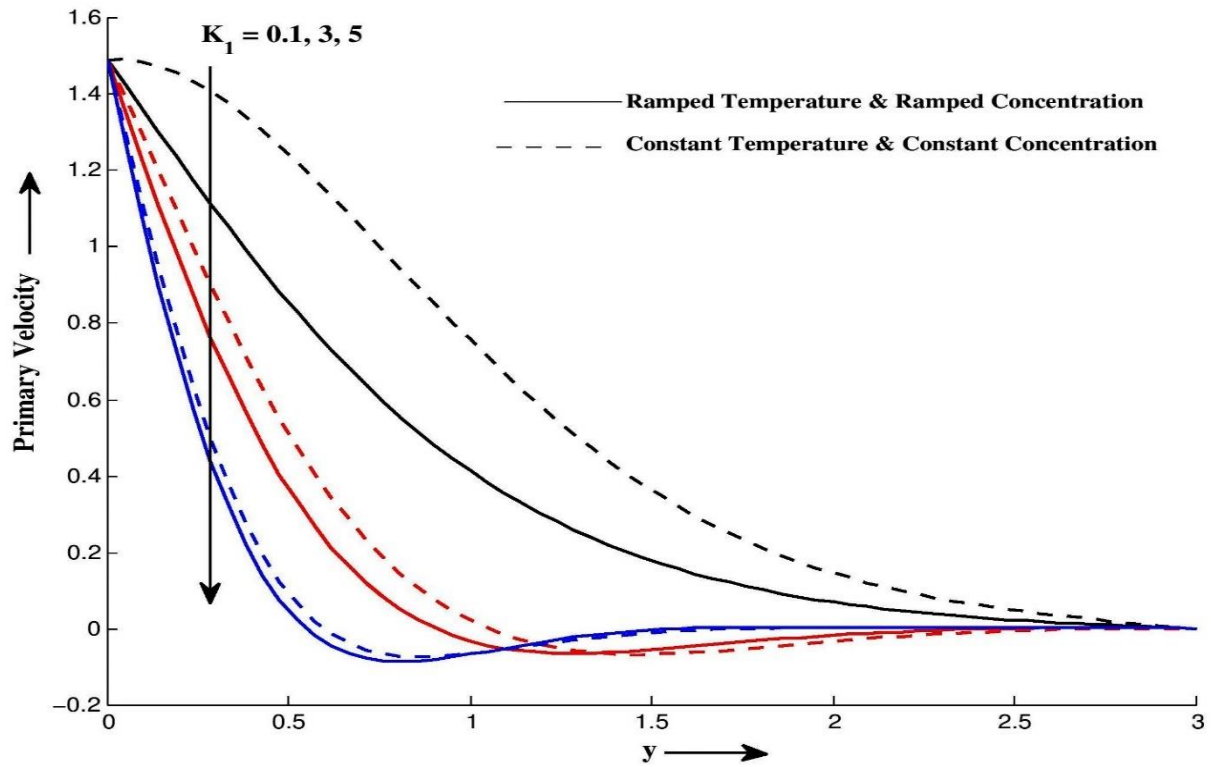


**Figure 7.2.10:** Primary Velocity  $u$  for different values of  $y$  and  $k_1$  at  $\gamma = 0.5, M = 5, k = 0.8, m = 5, Pr = 7, Sc = 6.2, H = 5, Gm = 10, Gr = 5, Nr = 5, Sr = 3, Kr = 5$  and  $t = 0.4$

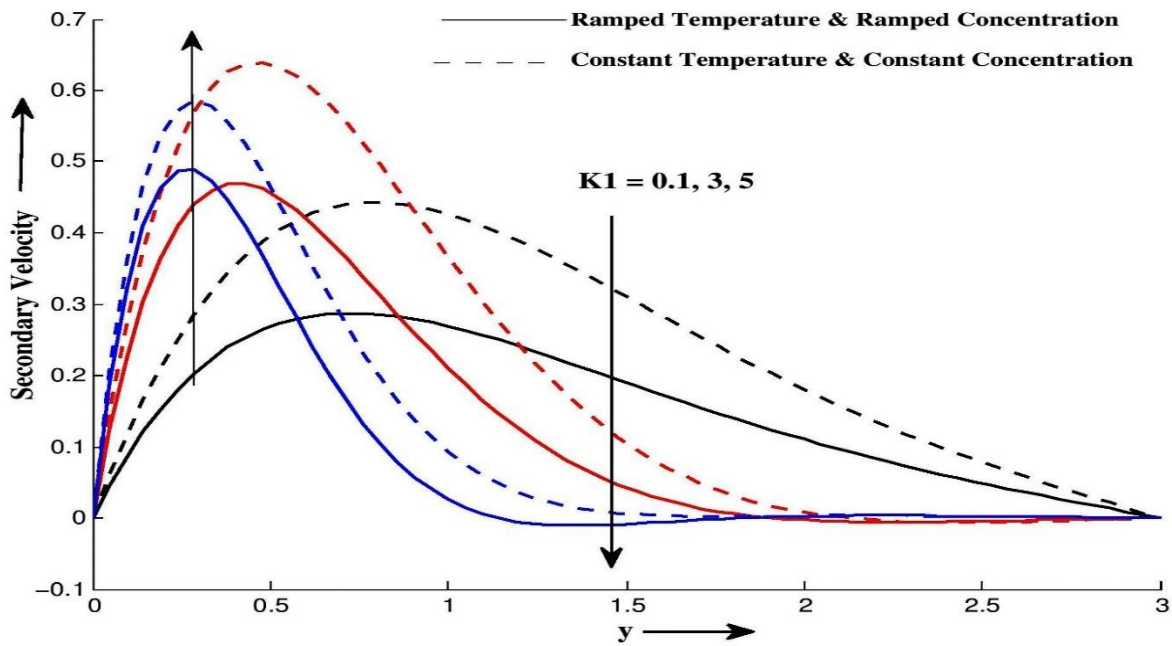


**Figure 7.2.11:** Secondary Velocity  $w$  for different values of  $y$  and  $k_1$  at  $\gamma = 0.5, M = 5, k = 0.8, m = 5, Pr = 7, Sc = 6.2, H = 5, Gm = 10, Gr = 5, Nr = 5, Sr = 3, Kr = 5$  and  $t = 0.4$

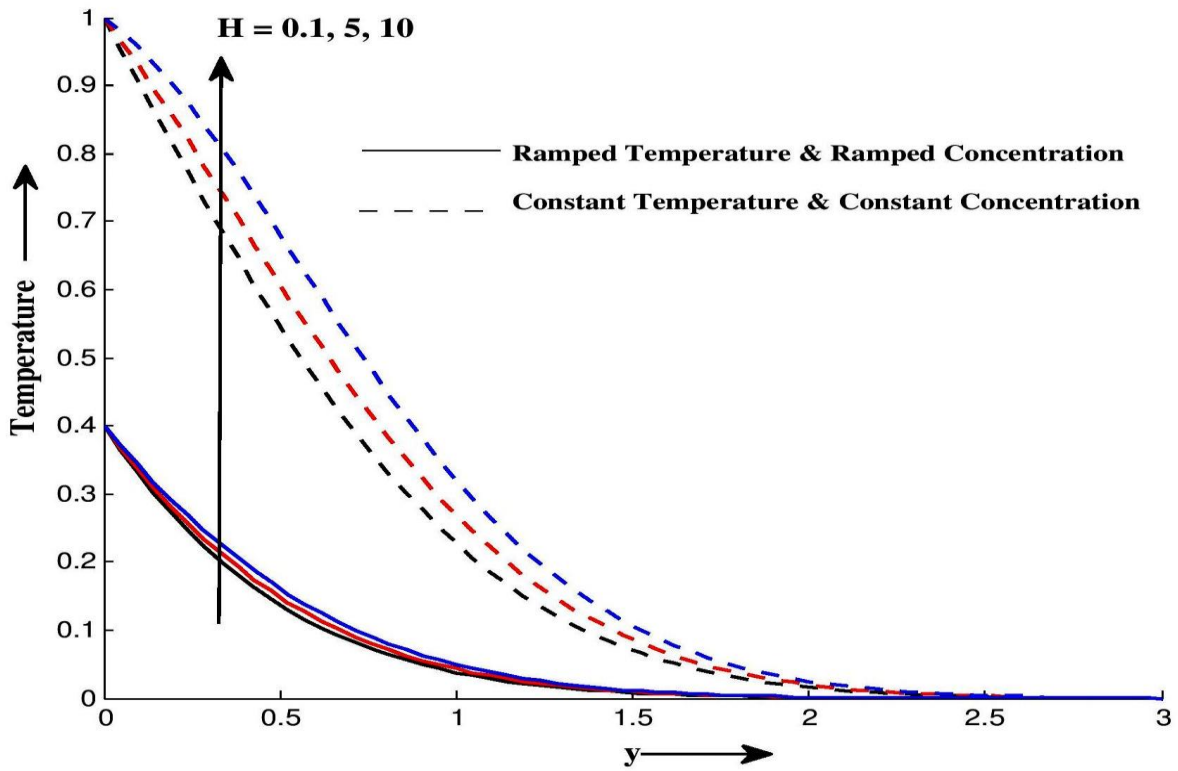


Figure 7.2.12: Temperature profiles  $\theta$  for different values of  $y$  and  $H$  at  $Pr = 7, Nr = 5$  and  $t = 0.4$

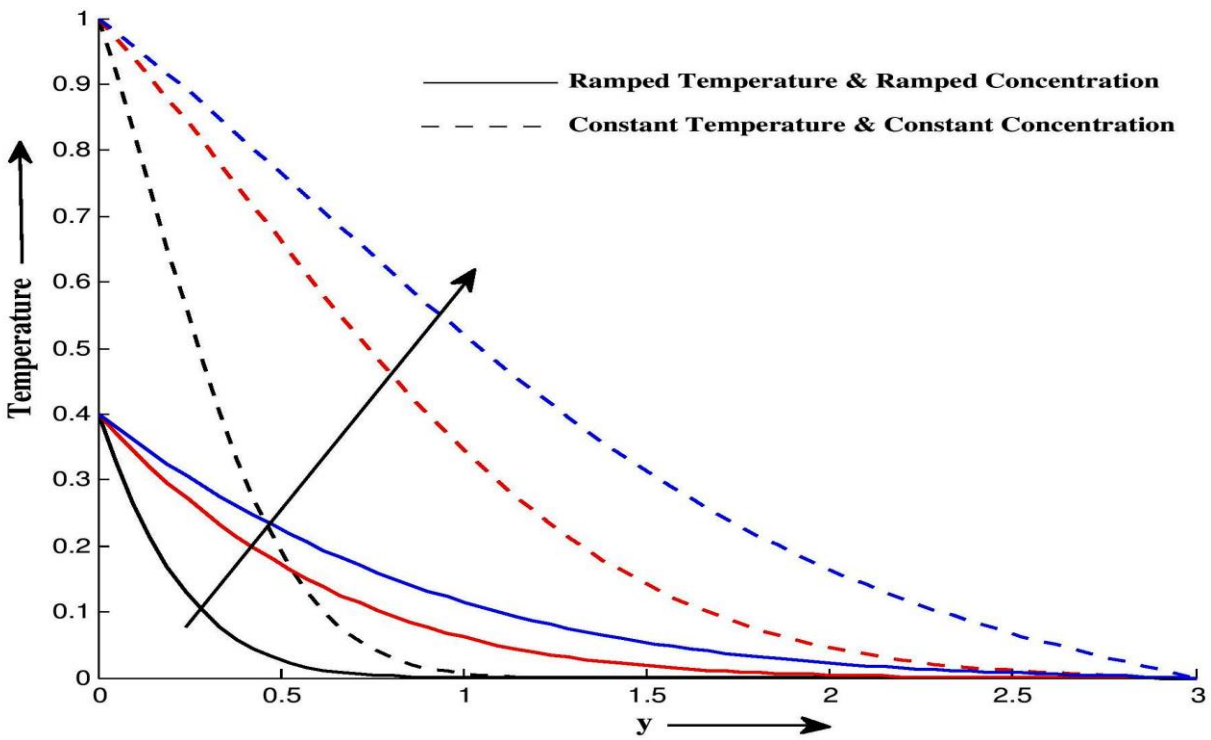
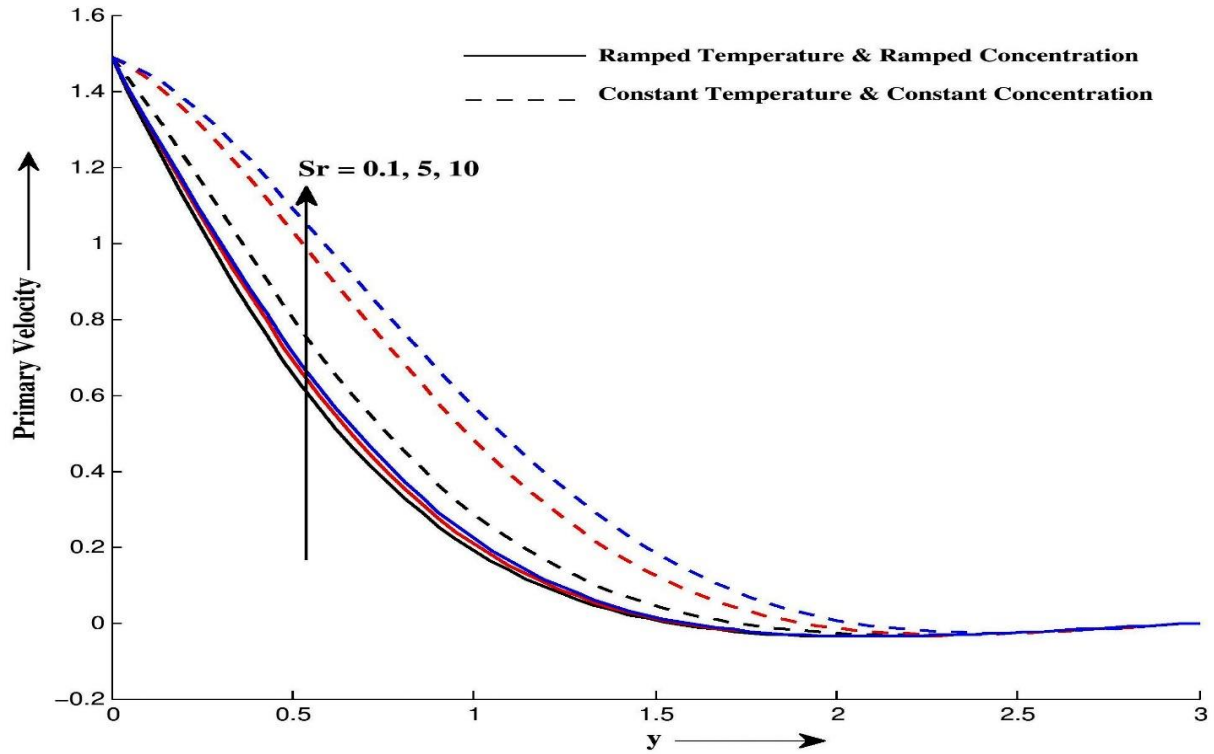
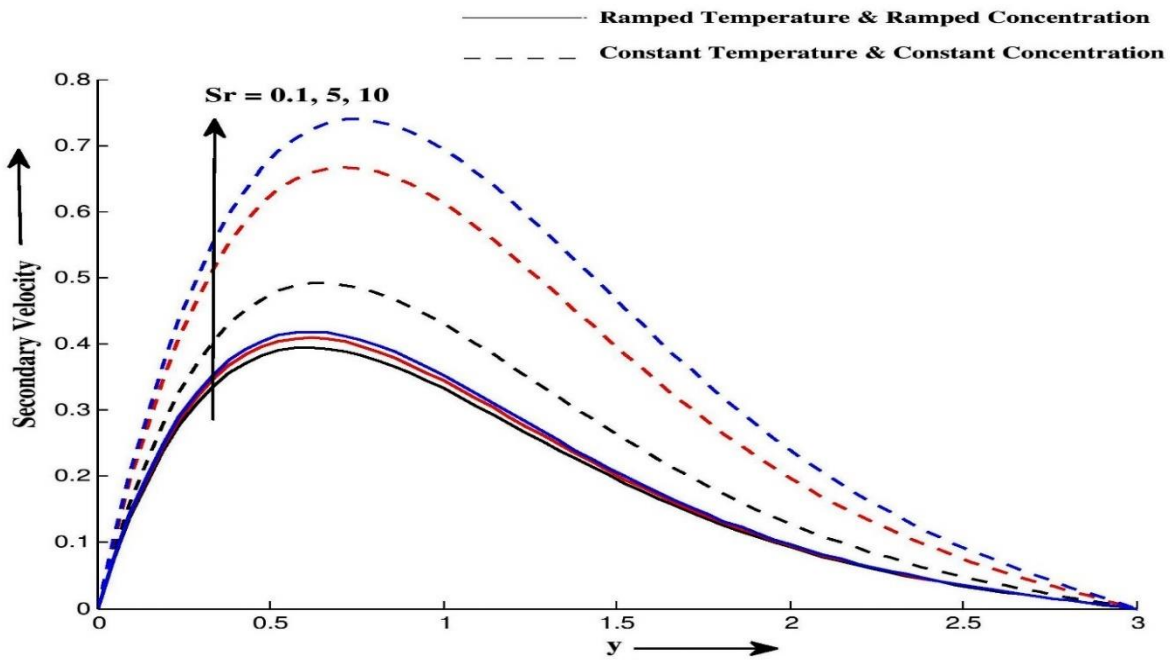


Figure 7.2.13: Temperature profile  $\theta$  for different values of  $y$  and  $Nr$  at  $Pr = 7, H = 5$  and  $t = 0.4$



**Figure 7.2.14:** Primary Velocity  $u$  for different values of  $y$  and  $Sr$  at  $\gamma = 0.5, M = 5, k = 0.8, m = 5, Pr = 7, Sc = 6.2, k_1 = 1.5, Gm = 10, Gr = 5, H = 5, Nr = 5, Kr = 5$  and  $t = 0.4$



**Figure 7.2.15:** Secondary Velocity  $w$  for different values of  $y$  and  $Sr$  at  $\gamma = 0.5, M = 5, k = 0.8, m = 5, Pr = 7, Sc = 6.2, k_1 = 1.5, Gm = 10, Gr = 5, H = 5, Nr = 5, Kr = 5$  and  $t = 0.4$

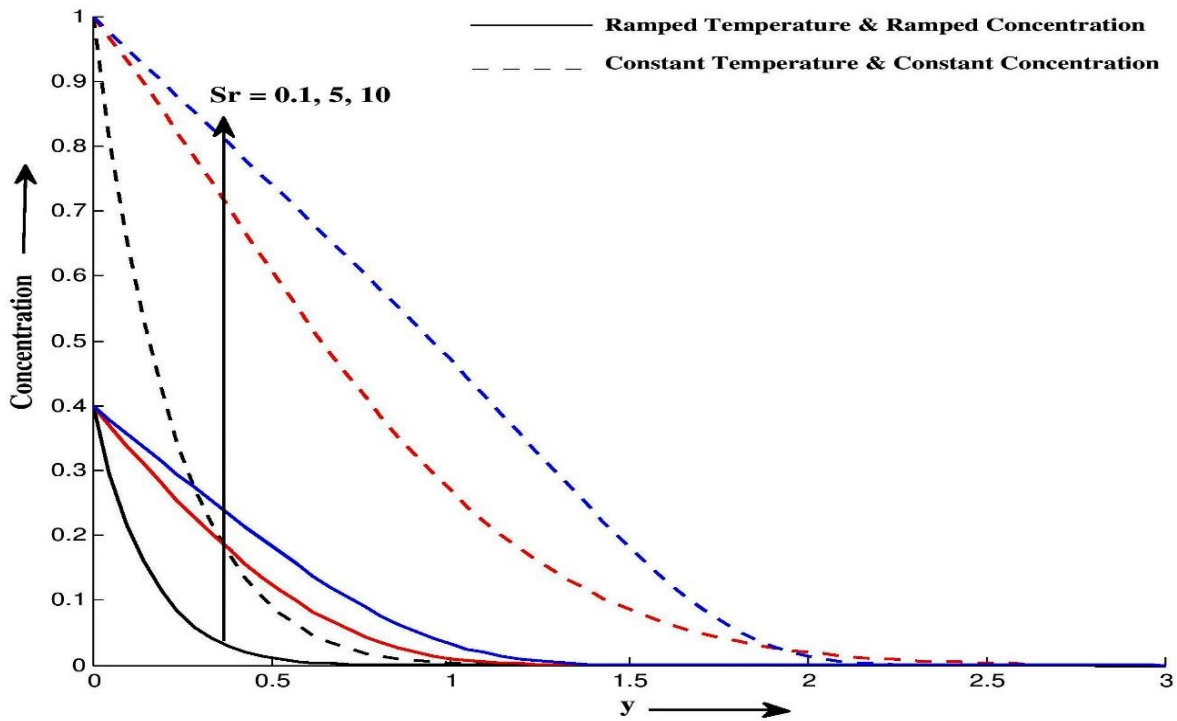


Figure 7.2.16: Concentration profile  $C$  for different values of  $y$  and  $Sr$  at  $Sc = 6.2, Kr = 5$  and  $t = 0.4$

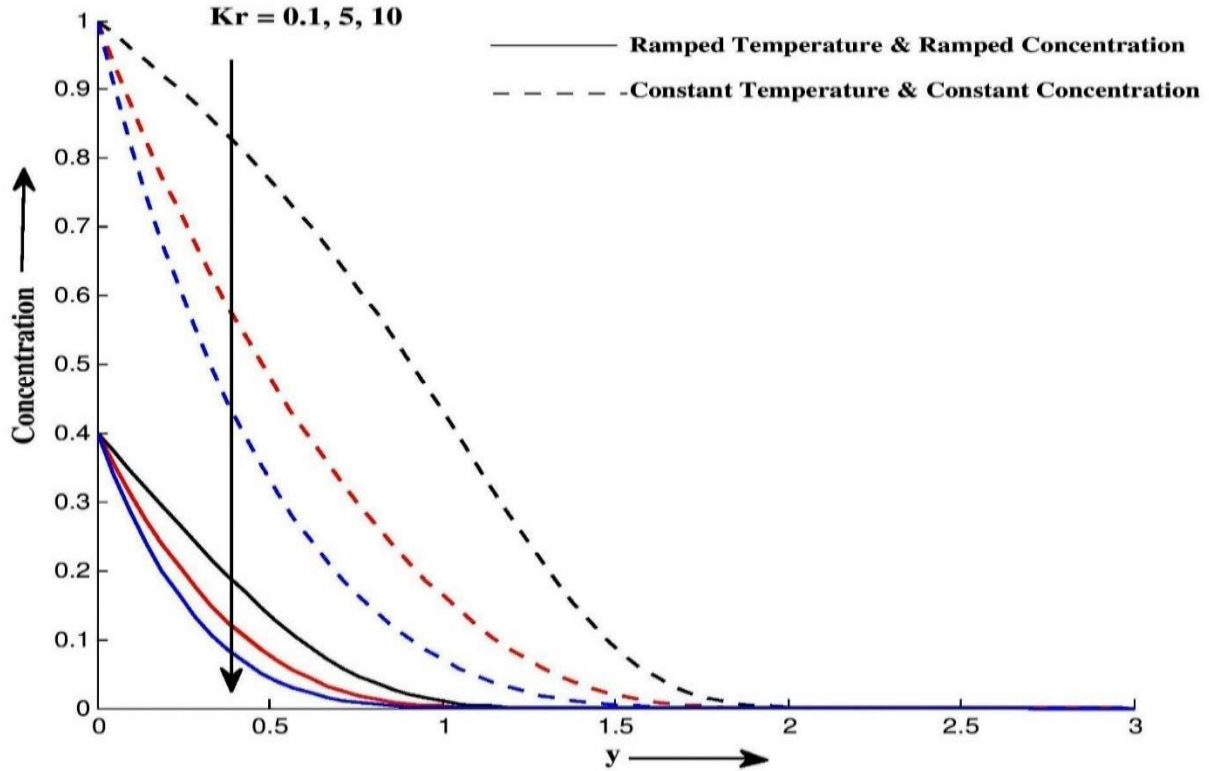


Figure 7.2.17: Concentration profile  $C$  for different values of  $y$  and  $Kr$  at  $Sc = 6.2, Sr = 3$  and  $t = 0.4$

Figure 7.2.6 and Figure 7.2.7 illustrate the impact of magnetic field parameter  $M$  on the primary and secondary velocities. Due to resistive Lorentz force effect on boundary layer, which reduces the motion of the fluid in  $x'$  direction, whereas magnetic field parameter tends to improve motion in  $z'$  direction. This result is important in MHD flow in rotating system. Figure 7.2.8 and Figure 7.2.9 show that primary and secondary velocities increase with increase in permeability of porous medium parameter  $k$ . Figure 7.2.10 and Figure 7.2.11 demonstrate the influence of rotation parameter  $k_1$  on the primary and secondary velocities. It is apparent from Figure 7.2.10, primary velocity decreases with increases in  $k_1$ . Figure 7.2.11 shows secondary velocity initially increase with increase in  $k_1$  for some intervals of direction  $y'$  after that velocity decrease with increase in  $k_1$ . Physically, Coriolis force created due to rotation, which is overturn fluid flow in the primary flow direction to induce secondary flow in the flow-field. Figure 7.2.12 illustrates heat generation/absorption effects on temperature profiles. These outcomes are obviously supported from the physical point of view because heat source indicates generation of heat from the surface of the region, which rises the temperature in the flow field. Figure 7.2.13 shows effect of thermal radiation on temperature profiles. Physically, when the amount of heat is generated through thermal radiation parameter increases which is improve fluid temperature. Figure 7.2.14 to Figure 7.2.16 show effect of thermo-diffusion on primary velocity, secondary velocity and concentration profiles for both boundary conditions. It is seen that thermo-diffusion tends to improve motion of the fluid in both direction  $x'$  and  $z'$  as well as concentration profile. Physically, intensification in values of Soret number raises the mass buoyancy force which results an increase in the value of velocity. Concentration profile for different values of chemical reaction parameter  $Kr$  are shown in Figure 7.2.17. It is evident that, chemical reaction parameter  $Kr$  tends to reduce mass transfer process throughout the flow field. This shows that the destructive reaction leads to decrease in the concentration field which in turn fails the buoyancy effects due to concentration gradients.

Table 7.2.1 to Table 7.2.3 show Skin friction, Nusselt number and Sherwood number for different physical parameters. It is seen that for both thermal cases magnitude of Skin friction increases with increase in Casson fluid parameter  $\gamma$  and decrease with increase in radiation parameter  $Nr$  and reaction parameter  $Kr$ . Skin friction increases in ramped temperature case while decreases in isothermal temperature case with increase in Soret number  $Sr$ . Magnitude of Sherwood number is rises with  $Kr$  and  $Sr$ .

**Table 7.2.1:** Skin friction Variation

$t$	$\gamma$	$M$	$K_1$	$Sc$	$Gm$	$Gr$	$Nr$	$Kr$	$Sr$	Skin friction $\tau =$ $\tau_x + i\tau_z$ for Ramped temperature	Skin friction $\tau =$ $\tau_x + i\tau_z$ for isothermal temperature
0.4	0.1	0.1	0.2	1	0.2	0.1	1.1	2	3	-11.3820	-13.8697
0.5	0.1	0.1	0.2	1	0.2	0.1	1.1	2	3	-13.8206	-15.3467
0.6	0.1	0.1	0.2	1	0.2	0.1	1.1	2	3	-16.1566	-16.9713
0.4	0.2	0.1	0.2	1	0.2	0.1	1.1	2	3	-8.0532	-10.7595
0.4	0.3	0.1	0.2	1	0.2	0.1	1.1	2	3	-6.2609	-9.5158
0.4	0.1	0.2	0.2	1	0.2	0.1	1.1	2	3	-11.4116	-13.8985
0.4	0.1	0.3	0.2	1	0.2	0.1	1.1	2	3	-11.4606	-13.9463
0.4	0.1	0.1	0.3	1	0.2	0.1	1.1	2	3	-9.5053	-12.1840
0.4	0.1	0.1	0.4	1	0.2	0.1	1.1	2	3	-8.2295	-11.2747
0.4	0.1	0.1	0.2	1.1	0.2	0.1	1.1	2	3	-10.6381	-14.0442
0.4	0.1	0.1	0.2	1.2	0.2	0.1	1.1	2	3	-12.1124	-14.2468
0.4	0.1	0.1	0.2	1	0.3	0.1	1.1	2	3	-9.8473	-14.5742
0.4	0.1	0.1	0.2	1	0.4	0.1	1.1	2	3	-8.3125	-15.2787
0.4	0.1	0.1	0.2	1	0.2	0.2	1.1	2	3	-13.6485	-14.1457
0.4	0.1	0.1	0.2	1	0.2	0.3	1.1	2	3	-15.9150	-14.4216
0.4	0.1	0.1	0.2	1	0.2	0.1	1.2	2	3	-11.4076	-13.9227
0.4	0.1	0.1	0.2	1	0.2	0.1	1.3	2	3	-10.9894	-13.9802
0.4	0.1	0.1	0.2	1	0.2	0.1	1.1	2.1	3	-11.5928	-13.8755
0.4	0.1	0.1	0.2	1	0.2	0.1	1.1	2.2	3	-11.8494	-13.8810
0.4	0.1	0.1	0.2	1	0.2	0.1	1.1	2	3.1	-11.2735	-13.9162
0.4	0.1	0.1	0.2	1	0.2	0.1	1.1	2	3.2	-11.1651	-13.9626

**Table 7.2.2:** Nusselt number variation

$t$	$Nr$	Nusselt number $Nu$ for Ramped temperature	Nusselt number $Nu$ for isothermal temperature
0.4	1.1	-0.0099	1.6008
0.5	1.1	-0.0138	1.4256
0.6	1.1	-0.0182	1.2957
0.4	1.2	-0.0097	1.5640
0.4	1.3	-0.0095	1.5296

**Table 7.2.3:** Sherwood number variation

$t$	$Nr$	$Pr$	$Kr$	$Sr$	Sherwood number $Sh$ for Ramped temperature	Sherwood number $Sh$ for isothermal temperature
0.4	1.1	7	2	3.2	-13.4681	-22.1708
0.5	1.1	7	2	3.2	-16.2478	-24.5394
0.6	1.1	7	2	3.2	-19.1657	-26.9464
0.6	1.2	7	2	3.2	-13.7344	-23.2219
0.6	1.3	7	2	3.2	-14.0347	-24.3845
0.6	1.1	7.1	2	3.2	-13.3908	-21.8807
0.4	1.1	7.2	2	3.2	-13.3182	-21.6069
0.4	1.1	7	2.1	3.2	-13.6615	-23.2075
0.4	1.1	7	2.2	3.2	-13.8584	-24.2542
0.4	1.1	7	2	3.3	-13.8712	-22.8411
0.4	1.1	7	2	3.4	-14.2742	-23.5113

### 7.2.6 Concluding Remark

Concluding remarks can be summarized as follows

- Thermo-diffusion  $Sr$ , Hall current  $m$ , heat generation  $H$ , permeability of porous medium  $k$  and thermal radiation  $Nr$  tends to improve motion of the fluid flow in both directions.
- Primary and Secondary fluid velocities decrease with increase in Casson fluid parameter  $\gamma$  and rotation parameter  $k_1$  for ramped wall temperature with ramped surface concentration.

- Chemical reaction  $Kr$  tends to retard effects on primary and secondary velocities.
- Magnetic field parameter  $M$  tends to reduced momentum in primary flow direction, whereas reverse effect in secondary flow direction.
- Heat transfer process increase with increase in thermal radiation  $Nr$  and heat generation parameter  $H$ .
- Mass transfer process delay with chemical reaction parameter  $Kr$ .